

# UC Berkeley

## Technical Completion Reports

### Title

Membrane Desalination of Agricultural Drainage Water: Water Recovery Enhancement and Brine Minimization

### Permalink

<https://escholarship.org/uc/item/926140wt>

### Author

Cohen, Yoram

### Publication Date

2008-01-05

# *Membrane Desalination of Agricultural Drainage Water: Water Recovery Enhancement and Brine Minimization*

Technical Completion Report SD001

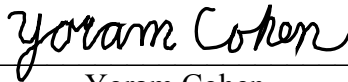
Submitted to

**UC Water Resources Center**

Rubidoux Hall-094  
University of California  
Riverside, CA 92521-0436

*by*

Principal Investigator



---

Yoram Cohen

Department of Chemical Engineering  
University of California, Los Angeles  
Los Angeles, Ca 90095  
Phone: (310) 825-8766; Fax: (310) 206-4107  
Email: [Yoram@ucla.edu](mailto:Yoram@ucla.edu);  
<http://www.watercenter.ucla.edu>  
<http://www.polysep.ucla.edu>

JANUARY 5, 2008

# TABLE OF CONTENTS

## Contents

TABLE OF CONTENTS.....	- 2 -
ABSTRACT.....	- 3 -
1. INTRODUCTION AND PROBLEM STATEMENT .....	- 4 -
2. OBJECTIVES .....	- 5 -
3. BACKGROUND .....	- 5 -
3.1 RO Desalting and Process Limitations .....	- 5 -
3.2 Integration of Chemical Demineralization with RO Membrane Desalting .....	- 8 -
4. PROCEDURES.....	- 11 -
4.1 Analysis of RO Recovery Limits.....	- 11 -
4.1.1 Field Water Site Selection for Sampling and Analysis.....	- 11 -
4.1.2 Recovery Limits.....	- 13 -
4.2. Experimental .....	- 14 -
4.2.1. Materials & Reagents.....	- 14 -
4.2.2. RO System .....	- 15 -
4.2.3. RO Mineral Scaling Tests.....	- 16 -
4.2.4. Calcium Removal by Accelerated Precipitation .....	- 16 -
5. RESULTS AND DISCUSSION .....	- 17 -
5.1 RO Product Water Recovery Limits.....	- 17 -
5.1.1 Analysis of RO Recovery Limits based on 1999-2003 Monitoring Data.....	- 17 -
5.1.2 Recovery Limits Determined for 2006-2007 Sampled Source Water Locations .....	- 24 -
6.0. Process Analysis and Laboratory Assessment of High Water Recovery via Integration of Accelerated Precipitation Softening with RO Desalination...-	31 -
6.1 Overview.....	- 31 -
6.2 High Recovery RO of Agricultural Drainage Water from the OAS Location.....	- 31 -
6.2.1 Recovery Limits.....	- 31 -
6.2.2 Overview of RO Process Simulations.....	- 33 -
6.2.3 Single Step APS-Membrane Desalting.....	- 34 -
6.2.4 Two-Step APS-Membrane Desalting .....	- 35 -
6.2.5 Antiscalant Effectiveness .....	- 39 -
6.2.6 Calcium Removal by Accelerated Precipitation Softening .....	- 40 -
6.3. Economic Feasibility of Two-Step Membrane Desalting with an Interstage Mineral Salt Precipitation.....	- 45 -
6.3.1. RO Desalination with Interstage Accelerated Precipitation Softening (OAS Water Source) .....	- 45 -
6.3.2. High Recovery Desalting Analysis for the LNW Source Water .....	- 48 -
6. CONCLUSIONS.....	- 50 -
7. REFERENCES .....	- 50 -

## ABSTRACT

Salinity of brackish groundwater in the San Joaquin Valley (SJV) is typically in the range of about 3,000 - 30,000 mg/L total dissolved solids (TDS). In recent years, there has been a growing interest in the potential use of membrane desalination technology for reducing the salinity SJV brackish water. Membrane desalination of SJV brackish water would have to be carried out at relatively high water recovery in order to reduce the volume of generated RO concentrate. However, at high water recoveries the concentration of mineral salt ions on the feed-side of the membrane may increase to levels that exceed the solubility limits of various sparingly water-soluble mineral salts (e.g., calcium sulfate, calcium carbonate, and barium sulfate). The ensuing crystallization of these minerals results in scale build-up that leads to permeate flux decline, shortening of membrane life, and thus a reduction in process efficiency and increased operational cost. Therefore, process strategies must be designed to enhance product water recovery, while reducing the potential for mineral salt scaling. Accordingly, the principal objective of the present study was to evaluate the feasibility of RO desalting of SJV brackish water.

The present project focused on a systematic evaluation of: (a) the recovery limits for RO desalination of SJV AD water that are imposed by mineral salt scaling, and (b) the integration of accelerated precipitation (AP) of mineral salts with RO desalting to mitigate scaling and enable high RO recovery. AP treatment would serve to demineralize and desaturate the RO primary or secondary feed with respect to mineral salt scalants. In the first phase of the project, a systematic analysis based on multi-electrolyte thermodynamic solubility calculations was carried out to determine the recovery limits due to mineral scaling. Subsequently, a detailed theoretical analysis and laboratory bench-scale studies were carried out with field water samples to assess mineral scaling propensity for a number of specific SJV water sources. In the second phase of the study, the integration of accelerated precipitation with RO desalting was investigated as a potential approach to lowering source water scaling propensity to enable enhanced water product recovery.

Analysis of historical water quality data and of recently obtained water field samples, from various locations in the San Joaquin Valley, demonstrated a significant variability of water salinity and scaling propensity with respect to calcite, gypsum, barite, and silica. The above analysis and experimental RO scaling tests suggested that the expected range of product water recovery by RO desalting across the SJV can be in the range of 50%-70% for most of the sites, with the exception of the ERR site for which a much higher recovery was estimated (in excess of 90%). The integration of accelerated precipitation with RO desalting was shown to be technically feasible for the range of brackish water quality in the San Joaquin Valley. In this process, the concentrate from primary RO (PRO) desalting would be treated by accelerated precipitation softening (i.e., chemical demineralization) or desaturated to lower the scaling propensity of this stream, followed by secondary RO (SRO) desalting. Overall recovery of up to ~90%-95% could be achieved at an estimated cost of \$0.56 - \$0.98 per m<sup>3</sup> product water, with the ACP process accounting for about 15%-25% of the overall water production cost.

The present study demonstrated provided a framework for assessing RO recovery limits and thus identifying potential hurdles that should be addressed in pilot studies and ultimately in the design and implementation of large-scale RO desalting processes. It is expected that, the methods developed in the present study for scale characterization, evaluation of accelerated precipitation effectiveness and RO process performance analysis will significantly advance the knowledge base needed to arrive at optimal design and deployment of future RO brackish water desalination strategies for the San Joaquin Valley.

# 1. INTRODUCTION AND PROBLEM STATEMENT

Rising salinity of agricultural drainage water and groundwater in the San Joaquin Valley (SJV), which now in the range of about 3,000-30,000 mg/L total dissolved solids (TDS), is a problem of growing concern [2-4]. Once the salinity exceeds the critical threshold, this once productive agricultural land may need to be retired, progressively diminishing the productivity of the SJV [2-5]. In order to reduce the buildup of salt in the soil, beginning in the late 1940s, surface and subsurface drains were installed in various regions of the SJV to collect brackish agricultural drainage (AD) water which was then diverted to evaporation ponds or other discharge sites [3]. Construction of a master drain discharging to the Sacramento-San Joaquin River Delta was halted in 1983 after the detection of high concentrations of selenium in the form of  $\text{SeO}_4^{2-}$  ion found at Kesterson - the site of a low-lying basin for tile drainage West Central San Joaquin valley [3, 4, 6]. The northern portion of the SJV has historically had natural drainage. The areas lacking natural drainage (e.g. Tulare Lake Bed and Kern Lake Bed), AD water may be sent to evaporation ponds and other discharge sites; however, bioaccumulation of selenium remains a major concern [3, 4, 6]. In such areas, water evaporation is a net loss of water that could be potentially be reclaimed and reused.

Reverse osmosis (RO) and nanofiltration (NF) membrane desalination can provide a viable technological approach of producing high quality water (for either agricultural reuse and/or potable water consumption). Membrane desalting can be achieved at remarkably low pressures with excellent product water flux and reasonably high levels of salt rejection. However, high salinity SJV drainage water (~3,000-30,000 mg/L) contains calcium, carbonate and sulfate ions at levels that are often close to saturation with respect to gypsum ( $\text{CaSO}_4 \cdot 2\text{H}_2\text{O}$ ), Calcium carbonate ( $\text{CaCO}_3$ ) and barite ( $\text{BaSO}_4$ ). At water recovery levels that are required to meet the recommended TDS level for agricultural water reuse (~750 mg/L), the concentration of mineral salt ions on the feed-side and near the membrane surface can increase to levels that will exceed the solubility limits with respect to the above and possibly other sparingly soluble mineral salts. The ensuing surface crystallization of these mineral salts and the deposition of their bulk crystals onto the membrane surface result in the formation of mineral surface scale. This leads to water permeate flux decline and potential damage to the membrane and thus shortening of its useful lifetime. Consequently, process efficiency is reduced and water production cost increases. It is also noted that, the composition of drainage water varies with time (with respect to salinity and the composition of sparingly soluble mineral salts) and correspondingly the mineral scaling propensity of such water is also time-dependent.

In order to assess the technical feasibility of RO desalination of SJV AD water, there is a need to evaluate the limits on product water recovery that are imposed by mineral salt scaling and osmotic pressure. Accordingly, in the present study, SJV AD water was first characterized with respect to composition, mineral salt saturation levels, and geographic and temporal variability. Based on RO process considerations (e.g. scaling and pressure), the upper limit on water recoveries, at different locations, were then estimated based on both thermodynamic solubility analysis and laboratory RO tests. The potential for enhancing RO recovery through the use of both antiscalants and interstage accelerated chemical demineralization (ACD) was then evaluated via a process simulations and laboratory bench-scale studies. The overall goal of the study was to provide quantitative data on the technical feasibility of RO desalting of AD water that could then be utilized for the design and deployment of pilot and full-scale RO desalting processes.

## 2. OBJECTIVES

The proposed research focused on evaluating the potential for integrating accelerated precipitation (AP) with membrane RO desalinating of San Joaquin Valley agricultural drainage (AD) water. The goal was to investigate the applicability of ADC for reducing the scaling propensity of AD water, thereby enabling enhanced product water recovery while avoiding the problem of membrane mineral scaling.

Given the variability of water quality in the San Joaquin Valley, it was important to quantify the range of achievable RO water recovery limits via conventional RO. This part of the study was accomplished by both theoretical thermodynamic solubility analysis and laboratory bench-scale studies with model solutions and field water samples to confirm the extent of scaling propensity of San Joaquin Valley AD water as well as the potential or RO integration with AP.

## 3. BACKGROUND

### 3.1 RO Desalting and Process Limitations

Membrane desalination is a promising technology for reducing the salinity of brackish agricultural drainage water in the San Joaquin Valley [7]. The typical arrangement for RO desalting (**Fig. 1**) uses a 2:1 array with the permeate product stream being the combined production from the first and second stages.

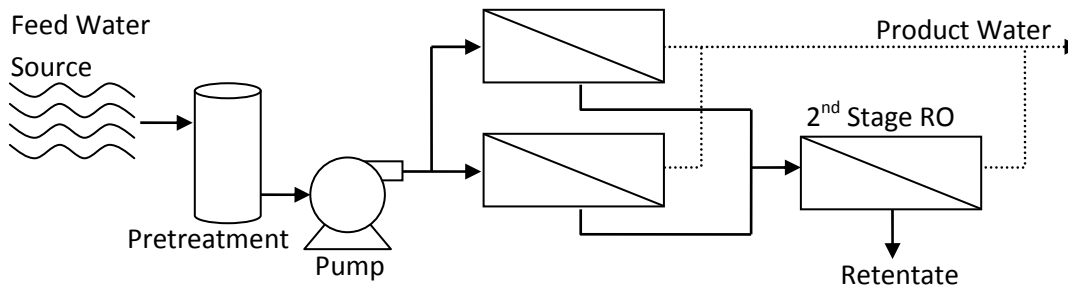


**Figure 1.** Typical arrangement of a 2:1 array RO desalting process. In this configuration, the largest percentage of permeate production is typically achieved in the first stage, while in the second stage the salinity is higher and thus permeate flux is typically lower. Various arrangements (e.g., with higher permeability second stage membranes) have been employed as well as operation where a booster pump is used between the first and second stage to increase the second stage pressure. Energy recovery devices are also used (not shown here) to recover energy from the high pressure retentate stream.

Fouling and scaling can lead to significant reduction in membrane performance (flux reduction and salt rejection impairment) and shortening of membrane life. While various feed pretreatment technologies have been advanced in recent years for the removal of particulate, bacterial and colloidal matter [3, 8-15], mineral salt scaling remains the major impediment to successful implementation of high recovery inland brackish water desalting. Studies have shown that membrane RO desalination of brackish groundwater from the San Joaquin Valley, with total dissolved solids (TDS) concentration in the range of ~3,000-30,000 mg/L, and the relatively low salinity Colorado River (CR) water (~700-1,300 mg/L TDS) are typically limited to product water recovery of about 50-60% [16-19] and 80%-90% [3, 16, 17, 20, 21], respectively, when

using conventional means of fouling and mineral scaling controls (i.e., acid and antiscalant dosing of the RO feed). The use of antiscalants adds to the overall cost of desalination (~5% - 15%), while the variability of water quality (especially with respect to feed water scaling propensity) makes it difficult to operate RO desalting with a sufficient degree of reliability.

As water permeates across an RO membrane, rejected salt ions accumulate near the membrane surface resulting in the formation of a concentration boundary layer. The concentration of the salts at the membrane surface can be approximated using the simple film model [22]:

$$CP = \frac{C_m}{C_b} = (1 - R_o) + R_o \exp\left(\frac{J}{k}\right) \quad (3.1)$$

where  $C_m$ ,  $C_b$ , and  $C_p$  are the concentrations of the solute at the membrane surface, in the bulk, and in the permeate, respectively,  $J$  is the permeate flux and  $k$  is the solute feed-side mass transfer coefficient,  $R_o$  is the observed rejection ( $R_o=1- C_p/C_b$ ), and CP is the concentration polarization modules. CP increases along the RO membrane channel, reaching its highest value at the channel exit [23]. As the concentration and osmotic pressure at the membrane surface gradually increase, from the entrance to the exit, the effective net driving force for permeation decreases, thus, the permeate flux decreases towards the exit region as illustrated in **Fig. 3.1a**.

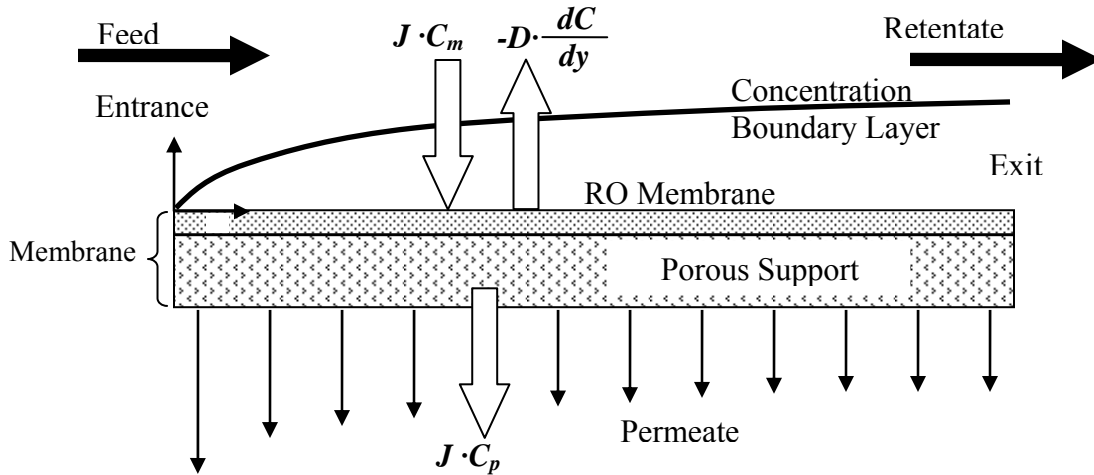


**Figure 3.1a.** Schematic of cross-flow plate-and-frame RO system showing the formation of a concentration boundary layer. Block arrow represent solute flux.  $J$  is the water flux,  $C_m$  and  $C_p$  are the respective concentrations at the membrane surface and in the permeate,  $D$  is the solute diffusivity, and  $dC/dy$  is the solute concentration gradient in the  $y$ -direction.

The observed salt rejection for an RO membrane,  $R_S$ , is defined as:

$$R_S = 1 - \frac{C_P}{C_F} \quad (3.2)$$

where  $C_P$  is the concentration of the permeate and  $C_F$  are the concentrations of the feed and permeate streams, respectively. Permeate productivity is measured in terms of the fractional recovery,  $R_W$ , defined as:

$$R_W = \frac{Q_P}{Q_F} = 1 - \frac{Q_R}{Q_F} \quad (3.3)$$

where  $Q_P$ ,  $Q_F$ , and  $Q_R$  are the permeate, feed, and retentate volumetric flow rates, respectively. The retentate stream becomes more concentrated with increased recovery and is concentrated by a factor,  $CF$ , defined as:

$$CF = \frac{C_C}{C_F} = \frac{1 - R_W(1 - R_S)}{1 - R_W} \quad (3.4)$$

where  $C_C$  and  $C_F$  are the respective concentrate and feed concentrations. As illustrated in **Fig. 3.1b**, the retentate stream is rapidly concentrated once the percent recovery begins to rise above about 85%. As a consequence, there is a corresponding rise in the osmotic pressure of the solution axially along the feed-side of the membrane. The osmotic pressure,  $\pi$ , is defined as

$$\pi = -\frac{(\mu_1 - \mu_1^0)}{V_1} \quad (3.5a)$$

where  $\mu_1$  and  $\mu_1^0$  are the osmotic pressure of the solvent in the solution and in its pure state, respectively, and  $V_1$  is the solvent molar volume. For dilute solutions can be estimated as,

$$\pi = CRT / M \quad (3.5b)$$

where  $\pi$  is the osmotic pressure (atm),  $C$  is the salt molar concentration,  $M$  is the molecular weight of the solute,  $R$  is the ideal gas constant ( $0.08206 \text{ L}\cdot\text{atm}\cdot\text{mol}^{-1}\cdot\text{K}^{-1}$ ), and  $T$  is the absolute temperature (K). For concentrated solutions and where non-idealities are important, the osmotic pressure may be calculated from more detailed thermodynamic expressions or with the use of available thermodynamic simulators [24].

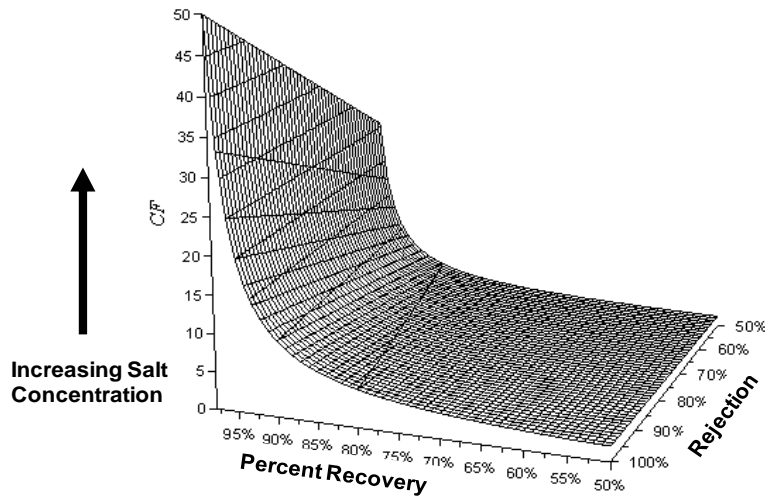


**Figure 3.1b.** Effect of product water recovery (percent recovery) and salt rejection on the level of concentration of the RO retentate (i.e., brine stream) relative to the feed.



Equation 3.4 can be rearranged such that the recovery can be found as a function of the concentration factor and the salt rejection:

$$R_w = \frac{CF - 1}{CF - 1 + R_s} \quad (3.5)$$

where  $R_w$  is the fractional product water recovery,  $CF$  is the concentration factor, and  $R_s$  is the observed fractional salt rejection. This equation can be used to estimate the expected recovery from small plate-and-frame RO cells by replacing  $CF$  in **Eq. 3.5** by the concentration polarization modulus,  $CP$ , from **Eq. 3.1**.

As recovery ( $R_w$ ) increases, the concentration of sparingly soluble mineral salts (e.g., calcium sulfate, calcium carbonate and barium sulfate) in the membrane channel can exceed their saturation limit leading to mineral salt precipitation and thus membrane scaling. The degree of saturation is typically expressed in terms of the saturation index which, for example, for calcite, gypsum and barite is defined as

$$\begin{aligned} SI_{calcite} &= (Ca^{2+})(CO_3^{2-}) / K_{sp_{calcite}} \\ SI_{gypsum} &= (Ca^{2+})(SO_4^{2-}) / K_{sp_{barite}} \\ SI_{barite} &= (Ba^{2+})(SO_4^{2-}) / K_{sp_{barite}} \end{aligned} \quad (3.6)$$

where  $(Ca^{2+})$ ,  $(Ba^{2+})$ ,  $(SO_4^{2-})$  and  $(CO_3^{2-})$  are the activities of the calcium, barium, sulfate and carbonate ions, respectively, and  $K_{sp_{calcite}}$ ,  $K_{sp_{gypsum}}$  and  $K_{sp_{barite}}$  are the solubility constants (products) for calcite, gypsum and barite, respectively.

### 3.2 Integration of Chemical Demineralization with RO Membrane Desalting

In order to enhance RO product water recovery, it is necessary to reduce the concentration of mineral scale forming ions below the scaling threshold. A two-stage process that integrates RO desalting with chemical demineralization is one of the technically viable solutions for achieving this goal [17]. In one configuration of this process, primary RO (PRO) desalting is carried out up to a product recovery level just below the membrane scaling threshold which is dictated by the source water quality, operating pH, and the type and dose of antiscalant used. The PRO concentrate stream is then chemically demineralized or desupersaturated (by an accelerated precipitation process) to lower the concentration of scale precursor ions, followed by a secondary RO (SRO) desalting of the treated PRO concentrate (i.e. PRO-ICD-SRO approach).

Several technologies that can potentially be applied for accelerated precipitation (AP) of treatment of the PRO concentrate have been proposed in the literature [25-39]. For example, the seeded reverse-osmosis process, developed for desalination of mine water high in calcium and sulfate ions [29, 30], utilized tubular RO membranes with the feed water seeded with calcium sulfate crystals. In the above process, as the feed-side stream was concentrated, accelerated gypsum precipitation is induced preferentially onto seed crystals, thereby minimizing crystallization onto the membrane surface. Excess crystals from the tubular RO concentrate were removed using a hydrocyclone, prior to recycling the seeded concentrate to the tubular RO feed tank. Although recovery levels in excess of 90% were reported, extensive laboratory and pilot plant studies demonstrated premature membrane damage (e.g. due to scouring) under

various operating conditions [30, 36]. It is noted that the above process requires specially designed tubular RO (or potentially NF) units that can accommodate suspended crystal, which could necessitate a significantly large footprint for large-scale applications. A similar process has been reported in which RO concentrate from desalting of dumpsite leachate was treated by [34, 35] by nanofiltration. NF was employed to generate solution supersaturation with respect to

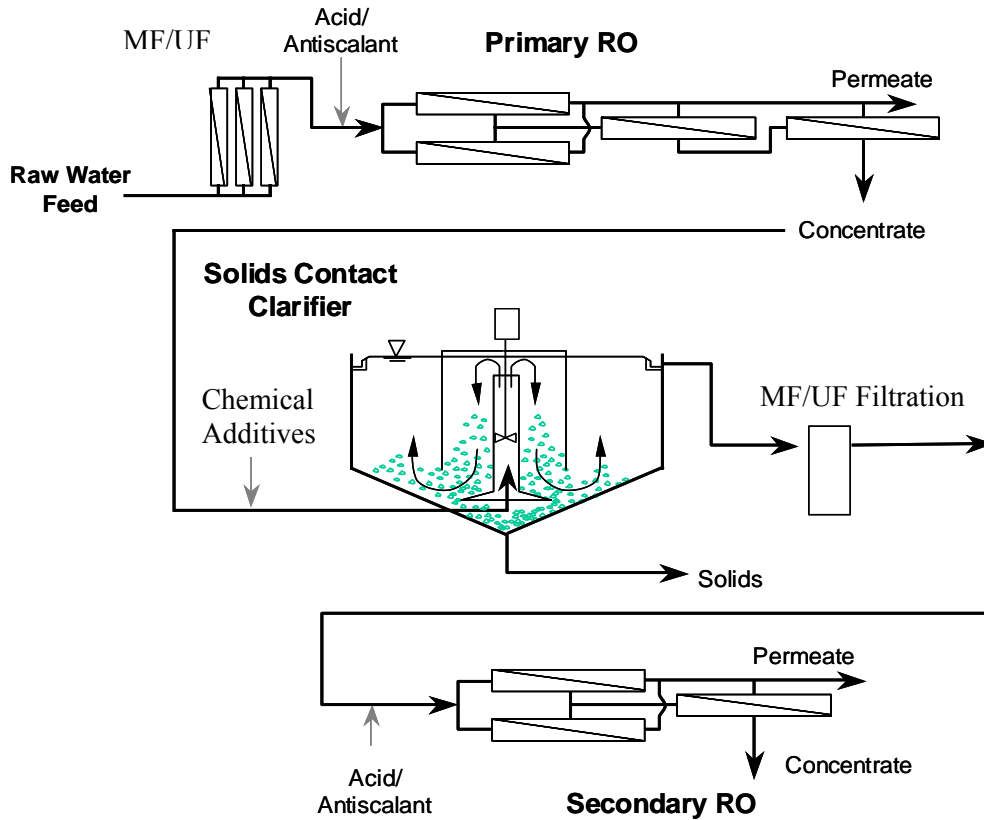


**Figure 3.2.** Schematic illustration of two-stage RO pilot-scale process

calcium sulfate; it is claimed that bulk precipitation did not occur within the NF modules, but occurred in a separate crystallizer unit. Despite the achievement of high overall desalination recovery (>95%), frequent NF flushing (every 30s) and alkali cleaning (every 250-300 hr) was required to mitigate fouling and/or scaling. There is limited experience and data for the above process and thus its potential applicability to other types of feed water is at present unclear.

The use of fixed-bed reactors to specifically mitigate barium sulfate scaling by desupersaturation of the primary RO concentrate was also reported in the literature [25, 26]. This approach, which was suitable for source water prone to barium sulfate scaling, relied on the existence of a wide metastable zone of barium sulfate (up to  $SI_b \sim 27$ ), which enabled primary RO desalting at relatively high water recovery. Prior to secondary RO desalting, the primary RO concentrate, which was supersaturated with respect to barium sulfate, was passed through a bed of barium sulfate seed crystals to desupersaturate this stream. Product water recovery above 90% was possible with the above process. However, early breakthrough of the packed bed occurred due to deactivation of seed crystals by adsorption of natural organic matter (NOM).

Accelerated precipitation (AP) by inducing calcium carbonate crystallization through chemical dosing (e.g., lime, caustic, soda ash) has been shown to be a promising approach for desupersaturation of primary RO concentrate [39]. This approach is analogous to the lime-soda

or caustic softening processes (i.e. precipitation softening), typically employed in central softening of municipal waters [40, 41]. The basis of the process is the strong pH dependency of calcium carbonate solubility that enables calcium carbonate precipitation through pH control. Conventional precipitation softening, however, is characterized by the production of fine suspension of mineral salt crystals that requires a long sedimentation time (about 1.5 to 3 hours). The resulting sludge is of low solids content (~2-30%), requiring extensive dewatering [40]. Due to the above shortcomings, alternative precipitation softening technologies have been developed to improve both precipitation kinetics and the efficiency of solid-liquid separation [28, 33, 37]. These technologies are based on the concept of seeded precipitation softening (SPS). Various studies have indicated that the use of crystal seeds in precipitation softening can provide a preferential surface area for heterogeneous nucleation and growth of mineral salts, thus accelerating the kinetics of mineral precipitation [25, 30, 33, 38, 42]. In addition, control of the initial seed size, loading and type provides a means of controlling the size of the final precipitates so as to facilitate efficient liquid-solid separation.

Variations of SPS reported in the literature include fluidized-bed type reactors [28] and systems with slurry recirculation through specially designed microfiltration units [27, 31, 32, 37]. Fluidized bed (pellet) reactors have been used for over a decade for central softening of municipal waters in the Netherlands [38]. In the above reactors, feed water and an alkaline solution are fed into a fluidized bed of sand particles that are typically 0.2 to 0.5 mm in size. Supersaturation of calcium carbonate is controlled such that precipitation occurs primarily by crystal growth onto the seeds (pelletization), producing compact pellets that can be easily gravity drained to yield a solid phase containing less than 10% water. It is noted that in the processes developed by Sluys et al. [37] and Kedem and Ben-Dror [31], in addition to seeded precipitation in a separate reactor, seed suspension was continuously re-circulated through a microfiltration unit. A transversal flow microfiltration unit was employed by Sluys et al. [37], with specially designed module hydrodynamics that minimizes fouling by seed crystal deposition. In the CAPS (Compact Accelerated Precipitation Softening) of Kedem and Ben-Dror [31], a calcium carbonate filter cake, in which rapid desupersaturation equilibration was achieved, served as a final “polishing” step for the product water, with periodic backwashing of the microfilter membrane unit.

The possible application of precipitation softening (PS) for the treatment of primary RO concentrate was discussed in a number of scoping studies [39, 43] that have suggested various conceptual process schemes to achieve high recovery. The above approach was recently demonstrated for high recovery desalting of relatively low salinity Colorado River Water. However, a comparable technical evaluation of the potential integration of accelerated precipitation treatment with RO desalting of AD water, which is the focus of the present study, has not been previously reported in the literature.

## **4. PROCEDURES**

### **4.1 Analysis of RO Recovery Limits**

#### ***4.1.1 Field Water Site Selection for Sampling and Analysis***

The first step in studying the feasibility of desalination of AD water in the San Joaquin Valley consisted of performing thermodynamic solubility analyses based on compositional data of water samples taken from different locations in the valley. The analyses were based on two data sets: (a) California Department of Water Resources (DWR) monitoring data for the period 1999 to 2003 for [44] collected from 55 sites, and (b) field water sampling data collected by DWR during 2006 – 2007 specifically for the present study. While the data from the DWR drainage monitoring reports contained sufficient information for selecting sampling locations, evaluating water quality variability, and determining recovery limits, the database lacked sufficient information on the concentrations of bicarbonate, carbonate, hydroxides, and silica. However, the DWR drainage monitoring data [44] did provide total alkalinity data. The more recent sampling carried out for the present project provided a more complete water quality data that enabled accurate determination of potential recovery levels by both theoretical analysis and via laboratory RO tests.

The first data developed by DWR [44] was analyzed to assess the temporal and geographical variability of water quality and the range of product water recovery limits for RO desalting. The analysis of recovery limits relied on solubility analysis performed using the OLI Systems Lab Analyzer 3.0 [24]. This simulator predicts thermodynamic properties of mixed electrolyte aqueous systems, including dissolved mineral salts' saturation indices which provide a measure of scaling tendencies. The data was further evaluated in order to select specific locations for sampling and laboratory bench-scale determination of RO recovery limits. Five specific sites were selected as being representative of the diversity of water compositions with respect to salinity (in terms of TDS), gypsum saturation index, and ratio of total carbonate to sulfate. The selected sites were readily accessible active sites from which field samples were obtained for the experimental part of the study. Water samples from these sites served for experimental confirmation of the potential RO recoveries, analysis of scaling propensity and feasibility studies on the potential integration of accelerated precipitation with RO for product water recovery enhancement.

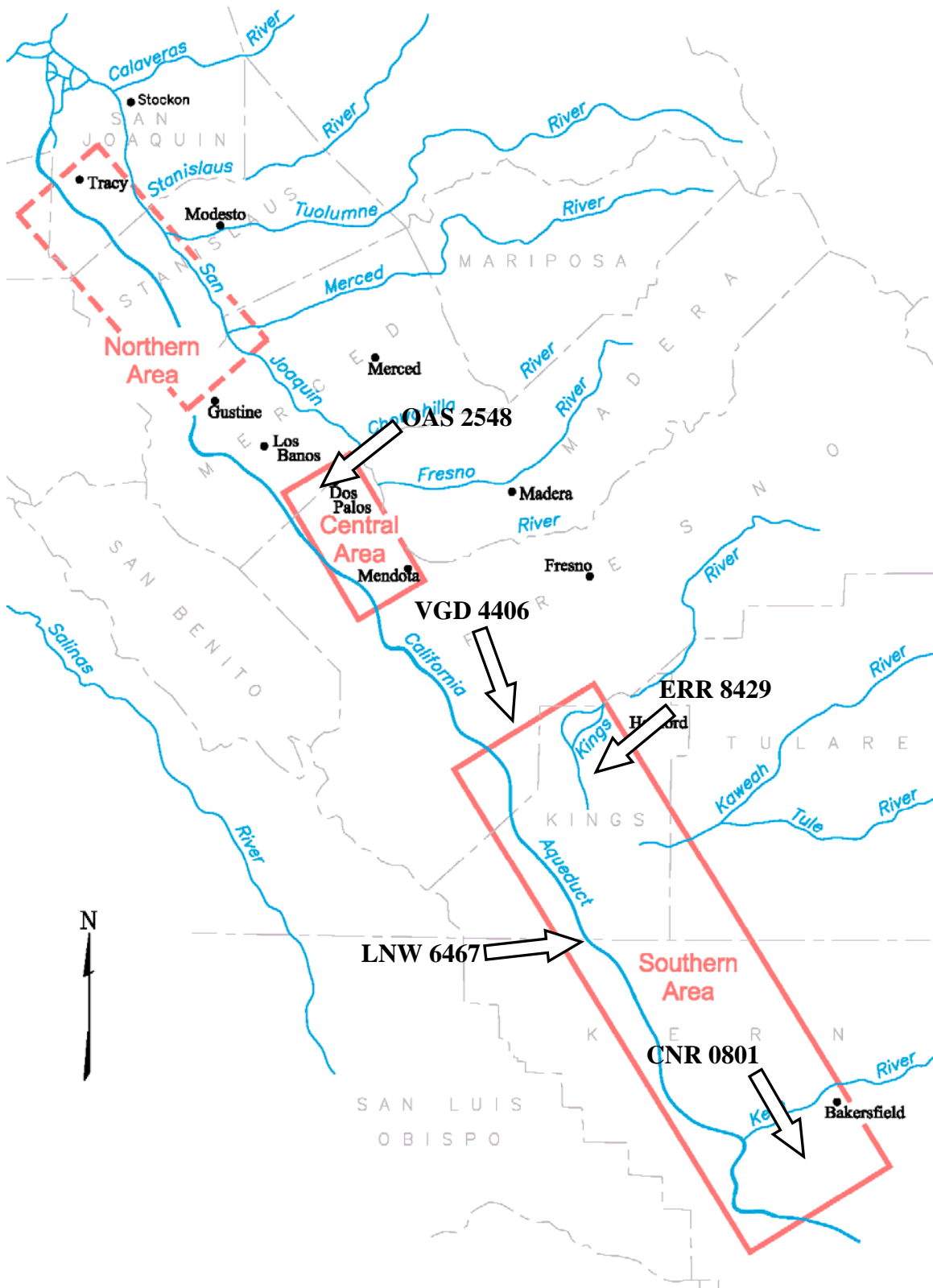


Figure 4.1. Field water sampling locations for RO recovery studies [3].

#### 4.1.2 Recovery Limits

RO recovery limits based on scaling were determined by calculating the recoveries at which the concentrations of sparingly soluble salts (e.g. calcite, gypsum, barite) reached their maximum controllable (i.e. non-scaling) saturation levels. Because of concentration polarization (CP), concentrations at the membrane surface can be significantly greater than in the bulk. Therefore, the SIs at the membrane surface were determined by multiplying the bulk ion concentrations by the average CP along the membrane and then calculating the SI values at these new, higher, concentrations. This approach accounts for changes in both ion concentrations and activities, but assumes that the level of concentration polarization is the same for all ions as given below,

$$SI_{m,i} = f\left(CP_{avg} \cdot \sum C_{b,j}\right) = \frac{IAP_{m,i}}{K_{SP}} \quad (4.1)$$

where  $SI_{m,i}$  is the saturation index at the membrane surface for the sparingly soluble salt,  $i$ ,  $CP_{avg}$  is the average concentration polarization along the membrane surface,  $C_{b,j}$  is the bulk concentration of ion,  $j$ , and  $IAP_{m,i}$  is the ion activity product at the membrane surface for sparingly soluble salt,  $i$ .  $CP_{avg}$  was estimated by the finite element numerical model developed by Lyster and Cohen [22] which considers the fully coupled governing equations for fluid dynamics and mass transfer. The saturation indices for calcite, gypsum, barite, and silica were calculated for a range of concentration factors (Eq. 3.4) to determine the recovery limits due to potential scaling. The calculated saturation indices were then plotted versus recovery (for a constant pH) by converting the retentate concentration factor to equivalent recovery using Eq. 3.5.

The scaling propensity of mineral salts found in AD water (expressed in terms the saturation indices) was determined from multi-electrolyte thermodynamic solubility analysis using the OLI Systems Stream Analyzer 2.0 [45]. Scaling of the primary scalants of concern was determined at the operating conditions (i.e., recovery and/or pH) at which the salts saturation indices exceed unity (Eq. 3.6). Calcite solubility increases substantially as the pH of the solution is lowered. Therefore, in RO processes, scaling by calcite can be typically mitigated by pH adjustment. Gypsum and barite saturation indices, however, are relatively pH insensitive and scaling by these salts cannot be managed by pH adjustment. Gypsum and barite precipitation can be inhibited to some degree when antiscalants are added to the RO feed. Scaling can generally be controlled for gypsum up to  $SI = 2.3$  and for barite up to  $SI = 90$  by using appropriate antiscalants [46]. Control of silica scaling is more difficult because of its speciation, formation of colloids, and potential polymerization in solution. Silica scaling can generally be controlled when its retentate concentrations are at or below the range of 160 – 240 ppm [47].

RO recovery limits were also estimated, via experimental RO desalting tests, for water from selected sampling locations in the San Joaquin Valley. Flux decline for desalting runs were quantified by plotting the relative flux (the flux at a given time divided by the initial flux) versus time. Average SI values at the membrane surface were calculated by first estimating the average CP for each run (Eq. 3.1) and then calculating the saturation indices (Eq. 3.6) at the new concentration by using the average CP. Equivalent recoveries were calculated, for each desalting test, using Eq. 3.5 by substituting  $CP_{avg}$  (Eq. 3.1) for  $CF$ . The above analysis for the experimental data, yielded an estimate of the recovery at which a commercial RO system would experience an average concentration in its exit region equivalent to that at the membrane surface in the plate-and-frame system,

$$R_{W,eqv} = \frac{CP_{avg} - 1}{CP_{avg} - 1 + R_s} \quad (4.3)$$

where  $R_{W,eqv}$  is the equivalent product water recovery,  $CP_{avg}$  is the average concentration polarization modulus (**Eq. 3.1**) at the membrane surface, and  $R_s$  is the observed salt rejection in the given experiment.

RO limitations could also arise from material limitations or process limitations with respect to the maximum allowable or acceptable operating pressure. For example, the common recommended pressure RO module ratings for seawater and brackish water RO modules are about 600 psi and 100 psi, respectively. Accordingly, the above limits place an upper bound on the osmotic pressure buildup in the RO process, which in turn sets the upper limit on the achievable product water recovery. Accordingly, in the present analysis recovery limits were also determined corresponding to the above two pressure limits.

## 4.2. Experimental

### 4.2.1. Materials & Reagents

Synthetic model solutions were prepared by dissolving reagent chemicals in de-ionized water obtained by filtering distilled water through a Milli-Q water system (Millipore Corp., San Jose, CA). Inorganic salts, obtained from Fisher Scientific (Pittsburgh, PA), were calcium chloride dihydrate (certified A.C.S.), magnesium sulfate heptahydrate (crystalline, certified A.C.S.), sodium chloride (granular, USP/FCC), sodium sulfate anhydrous (granular, certified A.C.S) and sodium bicarbonate (powder, certified A.C.S). Calcium carbonate (powder, 10 microns, 98%) and calcium sulfate dihydrate (98%, A.C.S. Reagent), both obtained from Sigma Aldrich (St. Louis, MO) were used as calcite and gypsum seeds, respectively, in the precipitation experiments. For pH adjustment, stock solutions of hydrochloric acid and sodium hydroxide were prepared from concentrated hydrochloric acid (22° Bé, technical, Fisher Scientific) and sodium hydroxide pellets (A.C.S. reagent, Sigma Aldrich), respectively. In some of the bench scale RO scaling and chemical demineralization experiments, antiscalant Flocon 260 (BioLab Water Additives, Lawrenceville, GA) or PC-504 (Nalco Company, Naperville, IL) were used for scale control. Agricultural drainage water field samples from five selected locations in the San Joaquin Valley were provided by the California Department of Water Resources (DWR) [48]. Upon delivery, the field water samples were refrigerated and maintained at 5°C prior to use.

Calcium ion potential and pH for grab samples were measured using a pH electrode (Cole Parmer Instrument Company, Vernon Hill, IL) and a calcium ion selective electrode (Orion 97-20, Thermo Electron Corporation, Somerset, NJ), respectively. Conductivity was measured using a conductivity meter (model WD-35607-30, Oakton Research, Vernon Hills, IL). Analyses of grab samples for metals, anions, alkalinity, total organic carbon (TOC), and silica were performed using methods published in Standard Methods for the Examination of Water and Wastewater [49] or using USEPA analytical methods for drinking water. Water quality data reconciliation and thermodynamic calculations, to obtain mineral salt saturation indices and solution osmotic pressure, were accomplished using LabAnalyzer 2.0 software (OLI Systems, Morris Plains, NJ), which is suitable for thermodynamic analysis of multi-ion aqueous solutions. Alkalinity and SDI of the field water samples were measured using the HACH model AL-DT

alkalinity test kit (Loveland, CO) and the Simple SDI Portable Auto SDI Tester (Applied Membranes, Inc., Vista, CA), respectively.

The aromatic polyamide RO membrane, LFC-1 (Hydranautics, Oceanside, CA) was selected for RO tests because of its low biofouling potential, high permeability, and high salt rejection [19]. The LFC-1 membrane has a permeability of  $9.8 \pm 0.3 \times 10^7 \text{ m bar}^{-1}\text{s}^{-1}$ , a nominal salt rejection of 98 %, and a root-mean-square (RMS) surface roughness of 65.5 nm [50]. Membrane compaction/conditioning was accomplished using solutions of sodium sulfate (certified A.C.S anhydrous, Fisher Scientific, Pittsburgh, PA).

#### 4.2.2. RO System

The diagnostic RO desalting system consisted of four main elements: a feed tank, a pump, two plate-and-frame reverse osmosis cells in parallel, and a microfiltration cartridge as shown in **Fig. 4.1**. A five-gallon polyethylene reservoir served as the feed tank for the water samples with temperature control provided through a refrigerated recirculator (model 625, Fisher Scientific, Pittsburgh, PA). The tank was placed on a stir plate and was stirred using a three-inch Teflon-coated stir bar. The feed pump was powered by a three-quarter horsepower electric motor (Dayton Electric Mfg. Co., Niles, IL) that drove a three-stroke positive displacement pump (Hydra-Cell, Wanner Engineering, Minneapolis, MN). A bypass valve allowed regulation of the feed flow rate to the reverse osmosis cells. All RO runs were carried out in a total recycle mode.

Two RO cells were arranged in parallel with each cell having an effective membrane surface area of  $19.8 \text{ cm}^2$  ( $2.6 \text{ cm} \times 7.6 \text{ cm}$ ). The permeate streams from both cells were combined and the permeate flow rate was measured using a digital flow meter (model 1000, Fisher Scientific, Pittsburgh, PA). The pressure in the cells was regulated by a backpressure valve (US Paraplate, Auburn, CA) placed following the recombination of the retentate streams. A rotameter (Blue-White Industries, Huntington Beach, CA) measured the flow rate of the retentate which was then filtered using a  $0.2 \text{ }\mu\text{m}$  Nylon filter cartridge (Cole-Parmer Instrument Company, Vernon Hills, IL).

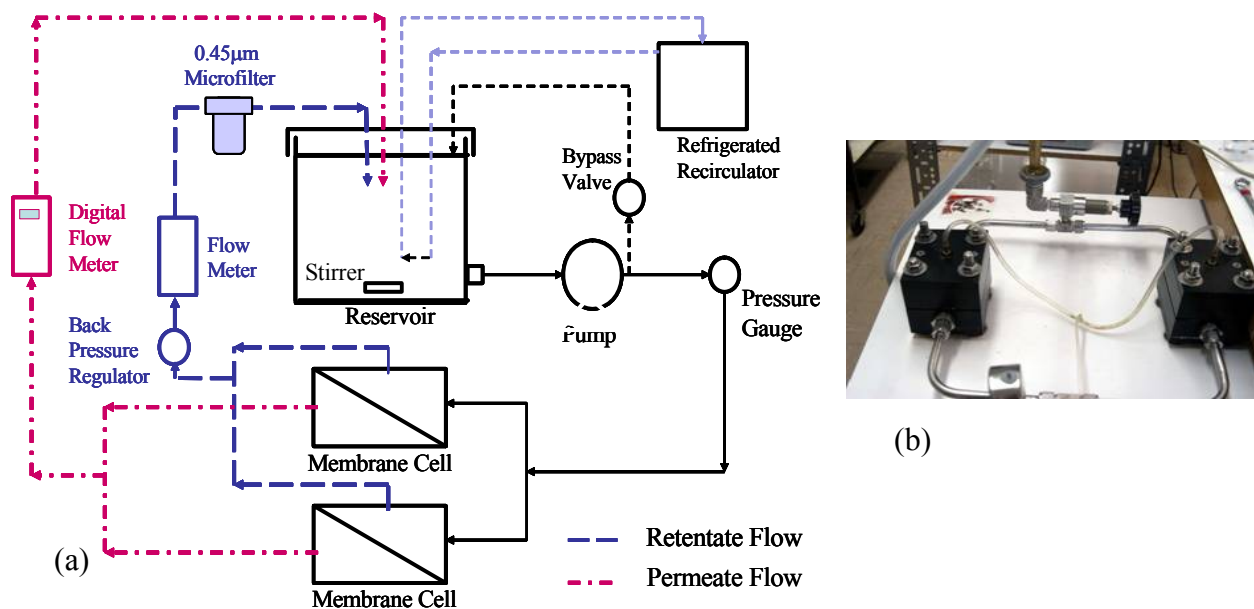


**Figure 4.1.** (a) Schematic of a plate-and-frame RO system. (b) RO cells arranged in parallel.



### 4.2.3. RO Mineral Scaling Tests

RO flux decline tests were performed with field water samples to assess the potential limitations on RO desalination imposed by mineral scaling. Scaling tests were carried out at the natural field water pH and also with adjustment to acidic conditions (pH range of ~5.3 - 6.5). Prior to each RO test, each field water sample was filtered successively through a 5  $\mu\text{m}$  gradient density polypropylene filter cartridge and a 0.2  $\mu\text{m}$  pleated Nylon filter cartridge (Cole-Parmer Instrument Company, Vernon Hills, IL) to remove suspended particles. In order to reduce pH drift during the experiments, air was bubbled through the water feed reservoir during pH adjustment to reduce the time required to reach equilibrium with respect to carbon dioxide. Some of the RO tests included scale control by antiscalant addition. All the flux data were expressed as a ratio of the flux  $F$  relative to the initial flux  $F_o$  (i.e., at  $t=0$ ).

Membranes used in the flat-sheet plate and frame RO cells were cut from a commercial stock membrane roll. The membrane coupons were rinsed with DI water to remove dirt and dust and subsequently soaked in DI water for at least two hours prior to placement in the RO cells. Prior to commencing with a desalting run, the membrane coupons were placed in the RO cells and conditioned by flowing through the RO system a sodium sulfate solution having approximately the same osmotic pressure as the field (or model) water solution. Membrane compaction was carried out at a retentate flow rate of about 4.5 L/min for an hour and then for 3 hours at retentate and permeate flow rates equal to the rates desired for the subsequent flux decline run.

After membrane conditioning, each flux decline run was initiated at the desired operating conditions (cross flow velocity of 0.11 m/s and permeate flow rate of 2 ml/min) for the specific feed water sample. All runs were carried out at the same initial flux and cross flow velocity in order to ensure that the all flux experiments are compared at about the same level of initial concentration polarization. At the end of the 24 hour flux decline the system was cleaned with DI water, followed by pH adjustment to 10 and using 0.1% v/v Micro-90, a concentrated detergent (International Products Corporation, Burlington, NJ), and also EDTA solution to remove traces of mineral scale, followed by rinsing with DI water.

### 4.2.4. Calcium Removal by Accelerated Precipitation

The extent of calcium removal by accelerated precipitation softening (APS) was conducted with a model solution representing the composition for feed water sample from the OAS site (**Tables 5.1**; see **Fig. 4.1**) as well as using field water samples from OAS and the LNW sites (**Table 6.2**). For each model solution type (feed and concentrate), multiple runs (~ 5) APS runs were conducted in 50-mL capped vials immersed in a temperature-controlled water bath (20°C), using a predetermined calcite seed loading and varying amounts of sodium carbonate or sodium hydroxide. At the termination of the APS treatment the solution was filtered using a 0.1-micron filter and the pH and the calcium ion potential were measured. In some of the experiments, when a larger sample volume required processing, a 600 ml crystallizer vessel or a larger 25 L laboratory crystallizer system was utilized (**Fig. 4.2**).

APS kinetics was initially assessed using a model solution (**Table 4.1**) representing the OAS water source. Precipitation reaction was carried out using 500-mL of the model solution in a 600 mL a magnetically-stirred beaker. The precipitation process was induced by dispersing a charge of calcite seeds, followed by the addition of a predetermined amount of either 1-M sodium carbonate or sodium hydroxide stock solution. Precipitation kinetics was followed by

continuous monitoring of both pH and calcium ion potential until steady was reached. Precipitation kinetic studies were also carried out with the actual field water samples from OAS and the LNW sites (**Table 5.2**)

**Table 4.1.** Composition of OAS-2548 source water based on 3/22/04 monitoring [1] and corresponding model solutions.

3/22/04 OAS Water Source		Model Solution	
Ions	Concentration (mg/L)		Concentration (mM)
Sodium	2,379	Na <sub>2</sub> SO <sub>4</sub>	49.28
Barium	0.5	MgSO <sub>4</sub> ·7H <sub>2</sub> O	9.15
Calcium	454	O	11.29
Potassium	10	CaCl <sub>2</sub> ·2H <sub>2</sub> O	0.73
Magnesium	223	NaNO <sub>3</sub>	2.91
Sulfate	5,630	NaHCO <sub>3</sub>	7.8
Chloride	847	pH	0.99
Nitrate	45	<i>SI<sub>Gypsum</sub></i>	3.98
Bicarbonate	178	<i>SI<sub>Calcite</sub></i>	95
TDS	9,703	<i>SI<sub>Barite</sub></i>	



**Figure 4.2.** Spiral-wound RO desalination system showing RO module and degassing membrane (to the right of RO module) and crystallizer/clarifier vessel.

## 5. RESULTS AND DISCUSSION

### 5.1 RO Product Water Recovery Limits

#### 5.1.1 Analysis of RO Recovery Limits based on 1999-2003 Monitoring Data

The 1999–2003 DWR monitoring data were analyzed with respect to seasonal and geographic variations in water quality and to determine potential recovery limits for different locations throughout the SJV. Five sample locations (CNR 0801, LNW 6467, OAS 2548, and VGD 4406) were selected for detailed thermodynamic solubility analysis and diagnostic flux decline experiments of field water samples. The analysis focused on the latest year of available data for each location because the most recent data are more likely to represent the current state of water quality in the SJV.

As illustrated in **Fig. 5.1**, AD water quality varied significantly over the course of a year for each of the selected location shown. As an example, the detailed water composition variability during different periods of the year for the OAS site in **Table 5.1**. It is clear that the saturation index with respect to gypsum was near or in the scale region ( $SI_g > 1$ ) for part of the 2003-2004 monitoring data shown in **Fig. 5.1**. Such water would be of high scaling propensity even at moderate recovery levels (less than about 70%). No consistent seasonal variations of water quality were found and there was no consistent correlation between the gypsum saturation index ( $SI_g$ ) and TDS. However, variations of  $SI_g$  appear to closely match changes in calcium concentration. The annual average TDS for the five sites ranged from about 6,987 mg/L to 23,480 mg/L for CNR and VGD, respectively, while the maximum absolute percent deviation of TDS from the average values ranged from 12% to 52% for LNW and OAS, respectively. The average calcium ion concentrations ranged from 356 mg/L to 606 mg/L for OAS and LNW,

respectively, and did not correlate with the low and high average TDS values. The maximum absolute percent deviation of calcium ion concentration from the average values ranged from 7.4% to 37% for LNW and OAS, respectively.  $SI_g$  varied from 0.75 to 0.99 (OAS and LNW, respectively), neither of which corresponds to the reported low or high TDS values. The maximum absolute percent deviation of  $SI_g$  from the average values ranged from 5.2% to 45% for CNR and OAS, respectively. The low and high values for average sulfate ion concentration, 4880 mg/L and 16,062 mg/L (LNW and VGD, respectively) do, however, correspond with the low and high average TDS values at these sites. The maximum absolute percent deviation of sulfate ion concentration from the average values ranged from 9.6% to 51% for LNW and OAS, respectively. Overall, OAS exhibited the greatest variability in water quality of the selected sites, while LNW exhibited the least variability.

**Table 5.1.** Selected examples of AD water quality in Location OAS2548 (Fig. 4.1)<sup>(a)</sup>

	Date				
	7/14/2003	9/9/2003	11/12/2003	1/12/2004	3/22/2004
	Composition (mg/L)				
Na <sup>+</sup>	1,810	1,080	2,320	2,830	2,310
SO <sub>4</sub> <sup>2-</sup>	3,990	2,340	5,550	6,460	5,630
TDS	5,864	3,828	9,344	11,100	9,576
Cl <sup>-</sup>	779	468	952	1,120	847
Total Alkalinity	271	239	160	173	146
HCO <sub>3</sub> <sup>-</sup>	330	290	195	211	178
EC	9,030	5,610	10,760	13,160	11,010
Hardness	1,362	988	1,793	2,099	2,052
Ca <sup>2+</sup>	283	224	385	430	454
Mg <sup>2+</sup>	159	104	202	249	223
K <sup>+</sup>	3.4	2.7	5	5	10
B	18.4	9.3	19.4	23	19.8
Ba <sup>2+</sup>	0.50	0.25	0.5	0.5	0.5
Se	0.1	0.06	0.14	0.17	0.15
pH	7.6	7.1	7.9	7.9	7.9
Temp, °C	22	21	18	14	15
Gypsum SI	0.57	0.41	0.83	0.94	0.98
Calcite SI	6.32	6.3	3.92	4.12	3.99
Barite SI	89.5	41	94.8	95.8	95.5

<sup>(a)</sup> DWR San Joaquin Valley Drainage Monitoring Program Database [51]; SI – saturation index, TDS – total dissolved solids (mg/L).

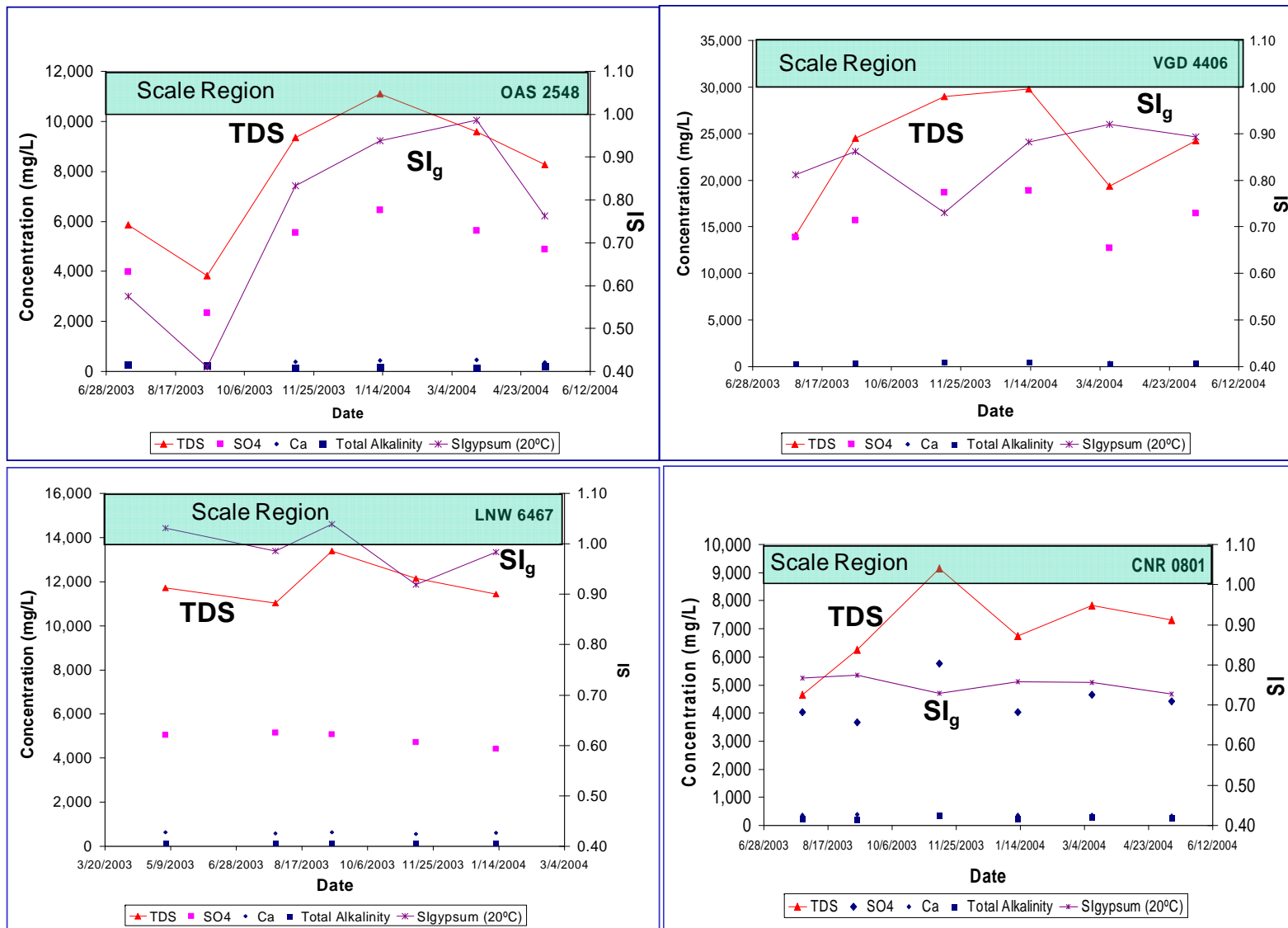


**Figure 5.1.** (a) Variability of water quality and saturation indices for gypsum and calcite (calculated using OLI [17, 45]) for brackish groundwater from several locations in the San Joaquin Valley. Data source: DWR San Joaquin Valley Drainage Monitoring Program Database [51].

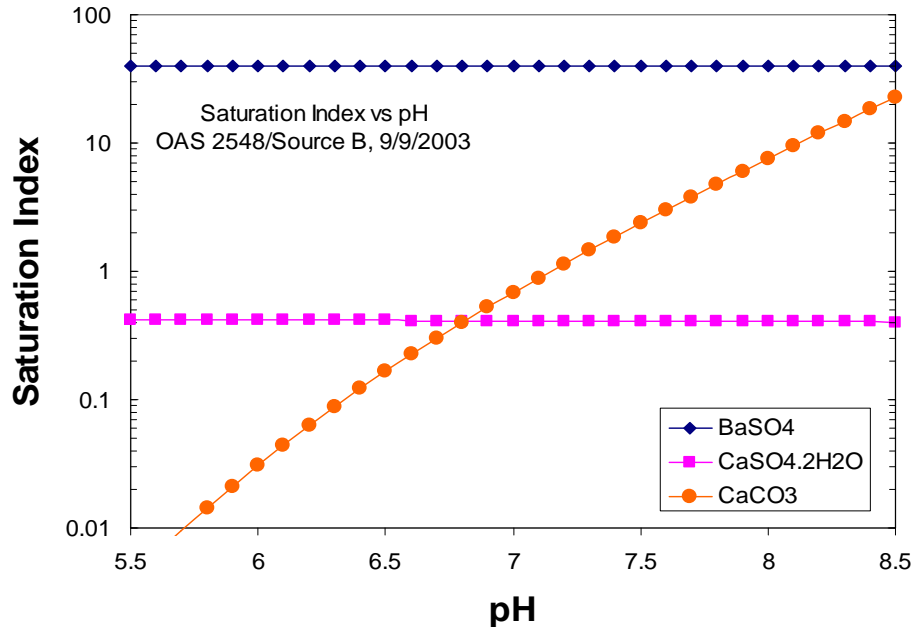


**Figure 5.2.** Saturation indices for calcite, gypsum and barite for the OAS-2548 location (Table 5.1).

The saturation index for calcite is highly dependent on pH as shown in the example of Fig. 5.2 for water from the OAS. For this water, calcite will precipitate once the pH exceeds about 6.8. However, calcite scaling can generally be managed by reducing the pH of the feed water. On the other hand the solubility of gypsum and barite are essentially pH independent. Therefore, different scale mitigation strategies are needed to combat gypsum and barite scaling as discussed later in this section (see also Section 6.25). It is noted that the saturation index plot for barite (Fig. 5.2) is included for illustrative purposes only given that barium concentrations were reported at or below the detection limits (i.e., 0.25 - 1.0 mg/L). The actual barium concentrations may be much lower, thus, the calculated barite saturation indices are upper limits.

The saturation indices for calcite, gypsum and barite were calculated for a range of concentration factors (Eq. 3.6) for the four locations (Fig. 4.1) to determine recovery limits. The change in SI with recovery was then calculated and plotted by converting the CF values to equivalent recoveries using Eq. 3.5. As an example, the variations of the mineral salt saturation indices with RO recovery are provided in Figs. 5.3a and 5.3b at pH of 7.5 and 6, respectively, for the VGD location for a condition of the highest TDS encountered in that location (~29,760 mg/L). It is clear that RO desalting would not be possible at pH of 7.5 given the supersaturation condition with respect to the three salts, calcite, gypsum and barite. Lowering the pH to 6, lowers the saturation index for calcite below unity; however, the feed water would remain supersaturated with respect to gypsum and barite. Another example is provided in Fig. 5.3 for desalting of water from the OAS site, during a time period in which the TDS was lowest (~3,828 mg/l). In this example, calcite would be supersaturated at pH of 7.5 but remains undersaturated upon reducing the pH to 6, while gypsum would remain undersaturated until one reaches a recovery level of about 58%.

Following the above analysis, product water recovery limits were determined as those at which gypsum or calcite saturation indices reached unity. This analysis was carried out for each of the four sample locations (**Fig. 4.1**) for conditions that were at lowest and highest TDS levels for the most recent year of available data at pH levels of 7.5 and 6.0 (**Table 5.2**). It is apparent that, for the locations listed in **Table 5.2**, RO desalting cannot be accomplished at pH=7.5 due to oversaturation with respect to calcite. At pH of 6, gypsum is the limiting scalant showing that in some cases RO recovery would be either infeasible or limited to low recovery, with the highest recovery of 53% for OAS2548 at the specific date shown. Barite scaling is not expected to be a limiting factor because, even though the water is oversaturated in barite. Experience has shown that the kinetics of barium sulfate precipitation is slow and typically not a major problem at the short residence times typically observed in RO desalination units [52-54].

**Table 5.2.** Recovery limits ( $SI = 1$ ) with respect to gypsum and calcite at pH = 7.5 and 6.0 for water samples having the maximum and minimum salinity for the latest year of reported data [44].

			Recovery Limits			
			pH =7.5		pH = 6.0	
Site	Sample Date	TDS (mg/L)	gypsum	calcite	gypsum	calcite
CNR 0801	11/12/2003	9,136	25%	0%	24%	86%
CNR 0801	7/28/2003	4,660	20%	0%	19%	88%
LNW 6467	9/9/2003	13,400	0%	0%	0%	86%
LNW 6467	7/28/2003	11,030	0.33%	0%	0.002%	87%
OAS 2548	1/12/2004	11,100	0%	0%	0%	93%
OAS 2548	9/9/2003	3,828	54%	0%	53%	90%
VGD 4406	1/13/2004	29,760	8.5%	0%	7.6%	91%
VGD 4406	7/29/2003	14,110	19%	0%	18%	92%

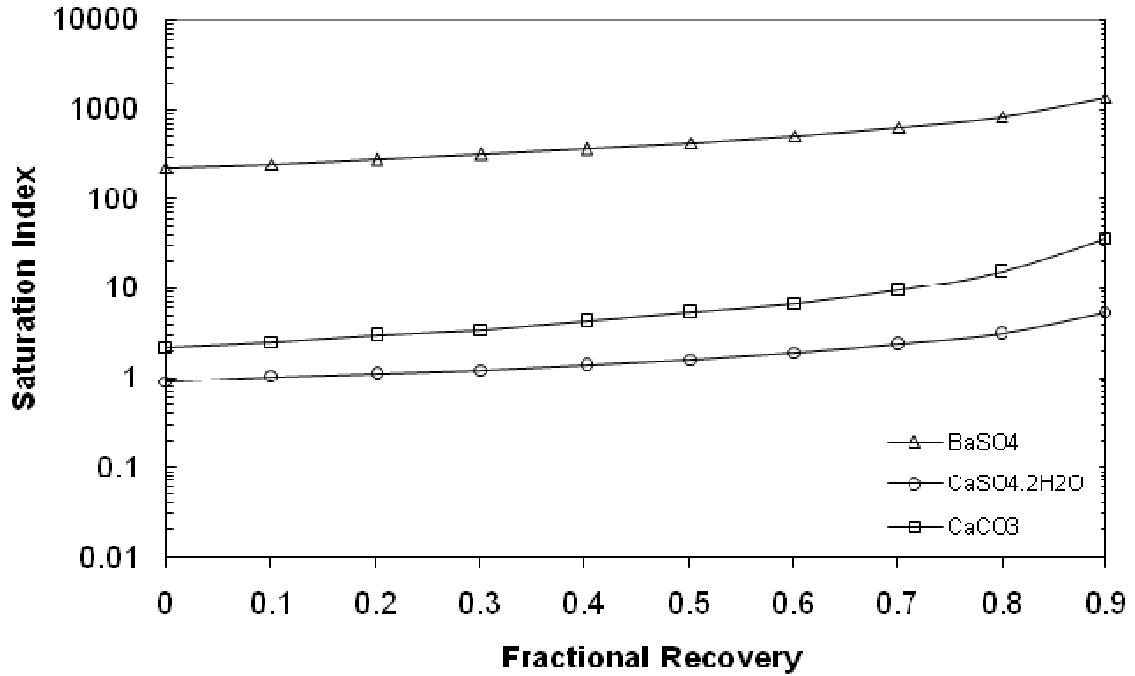


Figure 5.2a. Variation of mineral salt saturation indices with recovery (VGD, TDS 29760, pH 7.5).

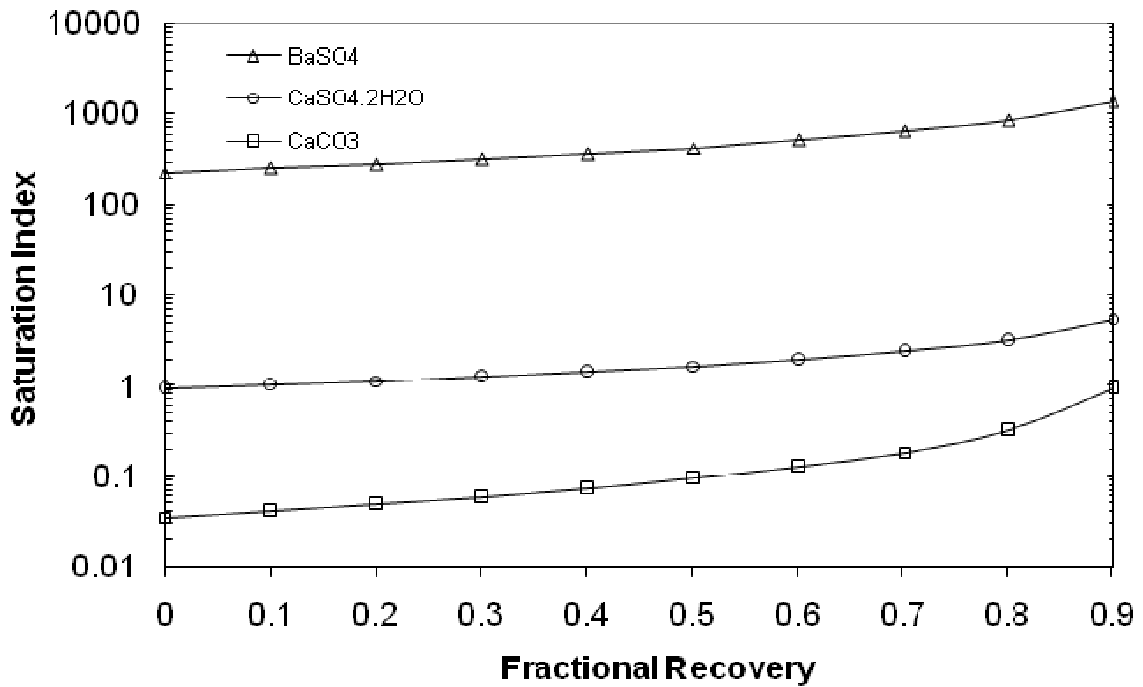


Figure 5.2b. Variation of mineral salt saturation indices with recovery (VGD, TDS 29760, pH 6.0).

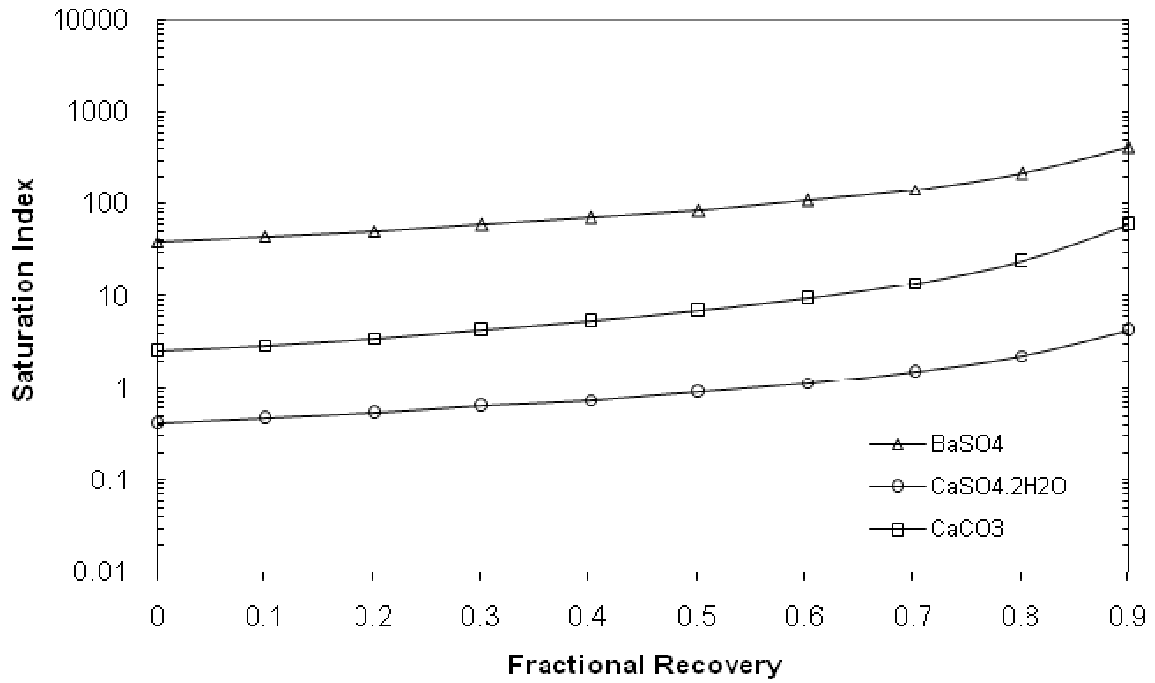


Figure 5.3a. Variation of mineral salt saturation indices with recovery (OAS, TDS 3828, pH 7.5).

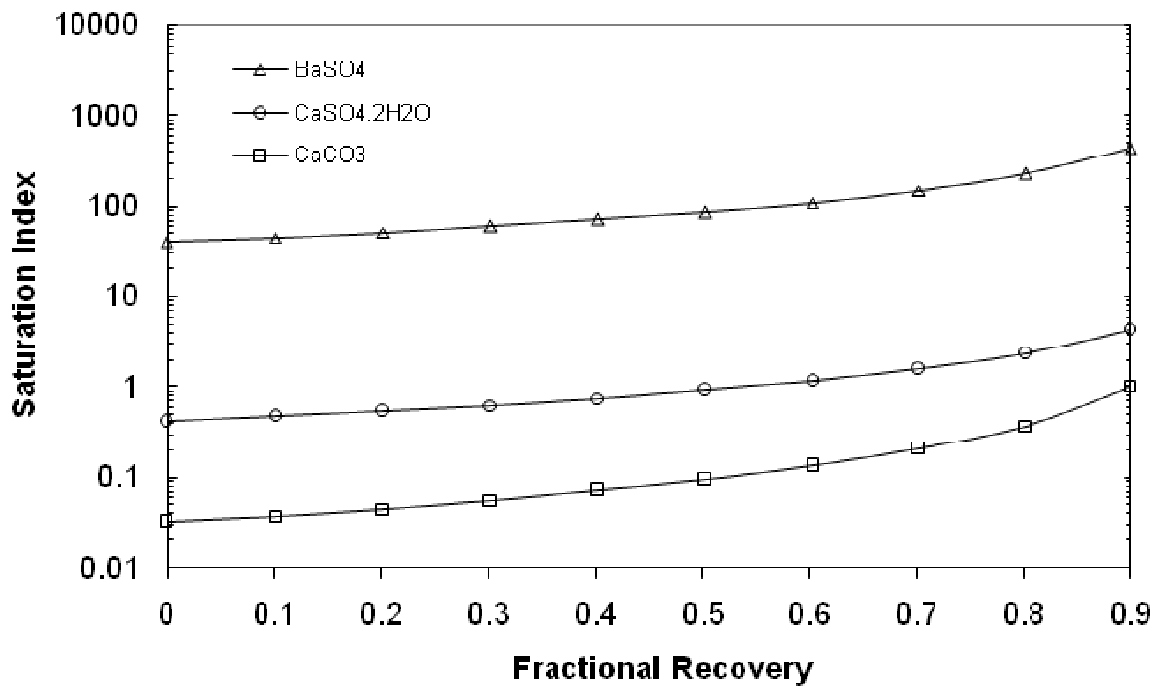


Figure 5.3b. Variation of mineral salt saturation indices with recovery (OAS, TDS 3828, pH 6.0).



### 5.1.2 Recovery Limits Determined for 2006-2007 Sampled Source Water Locations

In order to arrive at a more current evaluation of water quality and RO feasibility, samples of 25 gallons were obtained during the 2006-2007 period from the five sampling locations indicated in **Fig. 5.1**. A summary of the detailed water quality analyses for the five locations is provided in **Tables 5.2** and **5.3**. Unlike the 2003-2004 data, the 2006-2007 data included information on bicarbonate and silica and thus enabled a more precise analysis of the RO recovery limits.

**Table 5.2.** Detailed water quality analyses for selected sites for the 2006–2007 period<sup>(a)</sup>.

Measurement	Units	Location				
		CNR (7/31/06)	LNW (2/15/06)	OAS (4/10/06)	VGD (11/13/06)	ERR (1/29/07)
Conductance	µS/cm	7111	14430	12620	26070	5580
pH	pH units	7.5	7.6	7.6	7.6	8
UV Absorbance (254 nm)	absorbance/cm	0.126	0.094	0.13	0.178	0.587
Bicarbonate ( as CaCO <sub>3</sub> )	mg/L	229	128	212	367	699
Boron	mg/L	13.5	17.5	23.5	43.4	2.6
Calcium	mg/L	350	625	462	422	88
Carbonate (as CaCO <sub>3</sub> )	mg/L	1*	1*	1*	1*	7
Chloride	mg/L	324	3020	1060	1910	632
Fluoride	mg/L	5*	10*	10*	5*	5*
Magnesium	mg/L	236	198	284	962	59
Nitrate	mg/L	344	155	46.7	51.9	51.3
DOC	mg/L as C	4.2	4.6	5.1	6.2	15.8
Potassium	mg/L	46.7	5*	5*	7.8	3.5
Selenium	mg/L	0.032	0.223	0.184	0.05*	0.011
Silica	mg/L	23.5	37.9	31.4	43.2	38
Sodium	mg/L	1250	2820	2780	9270	1250
Sulfate	mg/L	3700	4520	6360	21400	1570
Total Alkalinity (as as CaCO <sub>3</sub> )	mg/L	230	128	213	368	706
Aluminum	mg/L	0.1*	0.1*	0.05*	0.5*	0.102
Arsenic	mg/L	0.01*	0.014	0.006	0.05*	0.089
Barium	mg/L	0.5*	0.5*	0.25*	2.5*	0.5*
TDS	mg/L	6372	11270	11020	28780	4115
Iron	mg/L	0.174	0.152	0.045	1.41	0.279
Manganese	mg/L	0.05*	0.05*	0.025*	1.55	0.595
TOC (as C)	mg/L	4.5	3.4	5.1	6.2	16.7
Phosphorus	mg/L	0.01*	0.03	0.08	0.12	1.96
Selenium	mg/L	0.034	0.235	0.195	0.05*	0.013
Strontium	mg/L	17.2	9.96	5.5	9.6	0.898
TSS	mg/L	1*	4	4	2	4

\* Reported value is at or below reporting limit. (a) Samples collected and analyzed specifically for present study.

**Table 5.3.** Field sample water quality and SI summary (2006–2007)

Name	Sample Date	Location	TDS, mg/L	pH	Total Alk, mg/L as CaCO <sub>3</sub>	SI <sub>C</sub>	SI <sub>g</sub>	SI <sub>s</sub>
CNR 0801	7/31/2006	Southern Area, Kern Lakebed	6372	7.5	230	2.70	0.704	0.222
LNW 6467	2/15/2006	Southern Area, Lost Hills	11270	7.6	128	2.72	1.03	0.345
OAS 2548	4/10/2006	Central Area	11020	7.6	213	3.02	0.985	0.287
VGD 4406	11/13/2006	Southern Area, Lemoore	28780	7.6	368	2.18	0.953	0.377
ERR 8429	1/29/2007	Southern Area, Corcoran	4115	8.0	706	9.50	0.120	0.339

**Note:** Values are those measured on the sampling date.

The variation of the saturation indices (including consideration of silica) with recovery for the recent water quality data (Tables 5.2 and 5.3) were determined, as described previously, in order to assess the recovery limit (i.e., at  $SI=1$ ). As an illustration, the results for the VGD and the OAS sites are provided in Figs. 5.4a and 5.4b, respectively, at pH of 6 and 7.6. The results clearly show that while calcite precipitation can be controlled with pH adjustment, gypsum remains the limiting scalant. It is also noted that silica scaling could be a problem at high recoveries (above about 70%). For both water sources, gypsum is oversaturated and thus desalting would require the use of antiscalants.

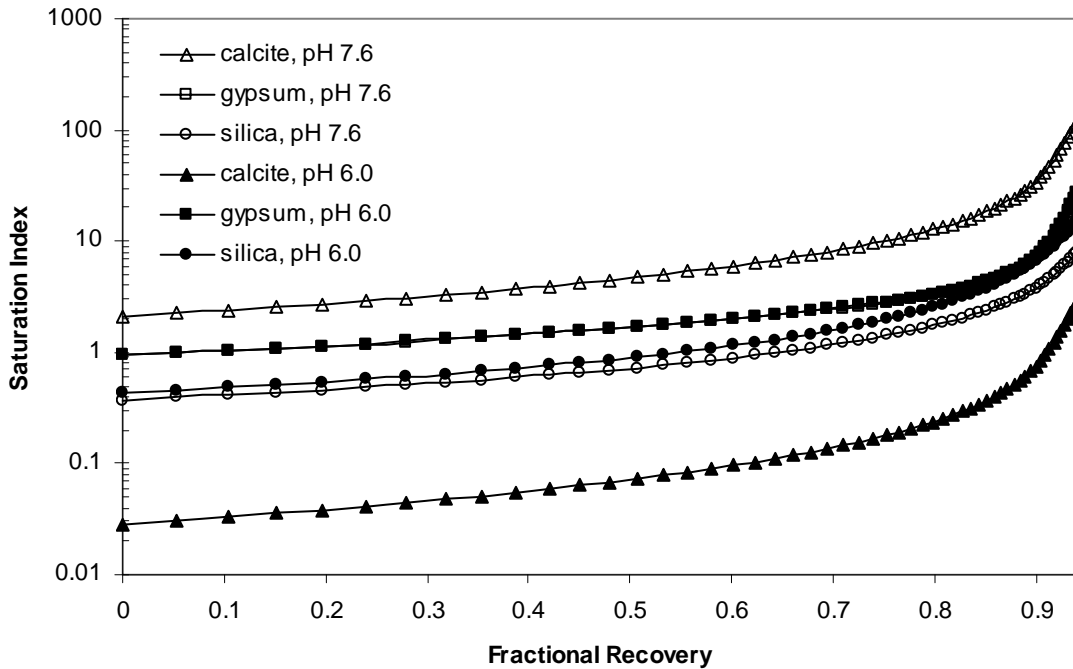


**Figure 5.4a.** VGD field water saturation indices as a function of RO recovery (see Table 5.2 for water quality data).

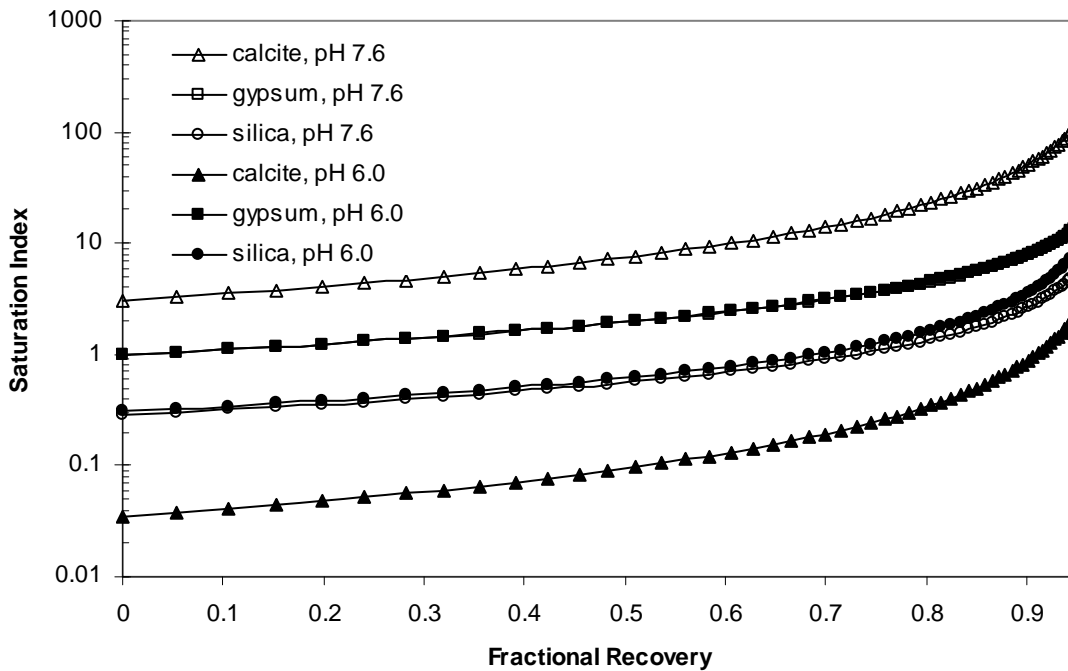


**Figure 5.4b.** OAS field water saturation indices as a function of recovery (see **Table 5.2** for water quality data).

A summary of the RO product water recovery limits, calculated based on the potential for scaling by gypsum, calcite, and silica for field water samples from each of the five sample locations (**Table 5.2**) is provided in **Table 5.4**. Calcite and silica recovery limits were calculated at the natural pH of the field samples and at pH of 6. The recovery limits due to gypsum scaling were determined for  $SI_g = 1$  and also at  $SI_g = 2.3$  which is typically the recommended limit for antiscalant scale control. Two possible osmotic pressure recovery limits (at 600 psi and 1000 psi) are also reported in **Table 5.4**.

**Table 5.4.** Recovery limits estimated based on water quality analysis of field water samples

Site	TDS, mg/L	Nat pH	Pressure Recovery Limits		Scaling Recovery Limits				
			Osmotic Pressure limit of 600 psi	Osmotic Pressure limit of 1000 psi	Calcite (natural pH)	Calcite (pH 6)	Gypsum (pH 6)	Gypsum <sup>(a)</sup> (pH 6)	Silica (pH 6)
					$SI_c = 1$	$SI_c = 1$	$SI_g = 1$	$SI_g = 2.3$	$SI_s = 1$
VGD	28,780	7.6	69.9%	81.4%	oversat.	91.1%	6.17%	67.0%	54.9%
ERR	4,116	8.0	94.3%	96.5%	oversat.	88.2%	85.3%	94.0%	63.4%
CNR	6,372	7.5	94.3%	96.5%	oversat.	91.0%	27.3%	68.2%	77.0%
OAS	11,020	7.6	88.9%	93.1%	oversat.	91.1%	0.70%	57.9%	68.9%
LNW	11,270	7.6	83.2%	89.6%	oversat.	90.0%	oversat.	53.6%	62.1%

**Note:** Bold values are the ultimate recovery limits with pH adjustment and antiscalant use.

<sup>(a)</sup> recovery attainable with the use of antiscalants for gypsum scale suppression.

The recovery limits as determined based on solubility analysis indicated that RO desalting would not be feasible at the natural source water pH (**Table 5.4**) due to oversaturation of with respect to calcite. However, upon pH adjustment to 6.0, the recovery limits increase to 88.2%–91.1%. However, gypsum would remain a limiting scalant imposing recovery limits that are unacceptable (below about 30%) for the VGD, CNR, OAS and LNW locations, with reasonably high recovery (~85%) feasible only for the ERR location. Antiscalant control of gypsum scaling (up to  $SI_g=2.3$ ) could enable recoveries in the range of about 54%-94% (**Table 5.4**). Silica can be the limiting scalant for the VGD and ERR sites imposing recovery limits of about 55% and 63 %, respectively. These limits are conservative as in RO practice one can often operate with silica concentrations up to about 100-200 ppm with the use of silica antiscalants. The recovery limits imposed by osmotic pressures of 600 psi and 1000 psi are in the range of 69.9%–94.3% (600 psi) and 81.4%–96.5% (1000 psi), respectively. It is noted that, even at the lower osmotic pressure limit of 600 psi, scaling remains a dominant recovery limiting factor.

It is important to recognize that the above analysis was based on thermodynamic solubility analysis and expected range of antiscalant effectiveness. Therefore, a more rigorous evaluation of scaling propensity was carried out via a series of flux decline experiments with field water samples from the five locations (**Fig. 4.1**). The evolution of the percent flux decline,  $FD = (1 - F_f / F_i) \cdot 100$  (where,  $F_f$  and  $F_i$  are the final and initial fluxes, respectively), was calculated for each experiment with the results at the end of the 24 hr test period provided in **Table 5.5**. The initial average SI values for calcite, gypsum, and silica, at the membrane surface ( $SI_{M,C}$ ,  $SI_{M,G}$ , and  $SI_{M,S}$ , respectively) were calculated based on the average concentration at the membrane surface estimating from the concentration polarization modulus (**Eq. 3.1**). The average CP values were estimated via a numerical concentration polarization model [22].

**Table 5.5.** Diagnostic flux decline experimental conditions and 24-hour flux decline

Site	Condition	TDS, mg/L	pH	x-flow, L/min	$F_i$ , $\mu\text{m/s}$	P, psi	$CP_a$ vg	$SI_{M,C}$	$SI_{M,G}$	$SI_{M,S}$	FD	$R_{w,eqv}$
VGD	Nat. pH	28,780	7.53	0.76	13.60	453	1.60	3.220	1.42	0.606	7.96 %	38%
VGD	Low pH	28,780	5.56	0.76	13.54	432	1.59	0.011	1.43	0.712	8.88 %	38%
VGD	Low pH+AS	28,780	5.93	0.76	13.60	455	1.61	0.045	1.44	0.720	9.36 %	38%
ERR	Low pH & AS	4,116	6.00	0.76	24.45	276	2.12	0.128	0.301	0.787	7.54 %	53%
ERR	Low pH	4116	5.37	0.76	24.43	306	2.12	0.010	0.307	0.786	11.6 %	53%
ERR	Nat. pH	4,116	8.02	0.76	24.46	302	2.13	29.300	0.280	0.678	12.4 %	53%
CNR	Nat. pH	6,375	7.50	0.76	24.41	278	2.11	7.370	1.53	0.464	6.37 %	53%
CNR	Low pH	6,372	5.27	0.76	24.44	270	2.11	0.006	1.55	0.487	11.0 %	53%
CNR	Low pH & AS	6,372	6.00	0.76	24.42	291	2.12	0.111	1.55	0.487	6.73 %	53%
OAS	Low pH & AS	11,020	5.94	0.76	24.36	349	2.11	0.862	2.10	0.660	7.89 %	53%
OAS	Low pH	11,020	5.47	0.76	24.46	374	2.1	0.0140	2.10	0.657	47.4 %	53%
OAS	Nat. pH	11,020	7.42	0.76	24.52	362	2.1	5.410	2.08	0.613	11.2 %	53%
LNW	Low pH	11,270	6.48	1.0	18.88	283	1.8	0.368	1.94	0.679	14.2 %	45%
LNW	Nat. pH	11,270	7.43	1.0	19.08	280	1.8	4.240	1.93	0.636	10.7 %	45%

**Note:**  $SI_{M,C}$ ,  $SI_{M,G}$ , and  $SI_{M,S}$  are the initial average saturation indices for calcite, gypsum and silica at the membrane surface; x-flow is the cross-flow velocity of the feed; P is the applied pressure;  $R_{w,eqv}$  is the equivalent recovery in the RO plant (**Eq 3.5**).

Equivalent product water recoveries for RO desalting based on the laboratory RO experiments was estimated based on **Eq. 3.5**. This estimate yields the recovery at which the average retentate concentration level, at the exit (module) from an actual RO plant, would be at equivalent to the concentration at the membrane surface in the plate-and-frame RO module. Accordingly, the equivalent operating recoveries (accounting for CP) were estimated to be 38% for VGD; 53% for ERR, CNR, and OAS; and 45% for LNW. It is noted that, the above estimates are for the best conditions achieved with the use of antiscalants as in the experimental tests. In these tests there was no observable scale but some flux decline (<5-10%) in some cases possibly due to residual membrane compaction. Thus, it is likely that higher recoveries could be attained either for the current or higher antiscalant dosages.

It is important to note that for RO tests that were performed without antiscalant addition, there was measurable flux decline and visible scale on the membrane surfaces at both the natural and pH adjusted cases (CNR, OAS, VGD, LNW). The ERR field water was the only sample undersaturated with respect to gypsum at the membrane surface for the present RO operating conditions. Overall, the results indicate that, with the exception of the ERR site, RO would not be feasible without antiscalants. For all of the field water except for VGD and ERR, there was significantly more flux decline at the lower pH than at the natural pH of the water samples. This behavior is exemplified by the results shown in **Fig 5.5a** and **5.5b**, for the OAS and CNR sites, respectively. The flux decline behavior was consistent with the level of membrane scale coverage as revealed in the images of **Figs. 5.6a** and **5.6b**, respectively. Contrary to conventional practice and assessment of scaling thresholds based on thermodynamic solubility analysis (**Table 5.4**), operating at higher pH (where the solution is oversaturated with respect to calcite) would be preferred to operating at lower pH. These results are consistent with a recent study [55] that reported that for SJV AD water, which is high in levels of sulfate and calcium (i.e., high gypsum scaling propensity) and lean in bicarbonate, low pH conditions result in suppression of calcite scaling by the sulfate ion and suppression of gypsum crystallization by the carbonate ion [55]. When operating at lower pH, antiscalant addition would improve the operating by suppressing scale formation, although at the expense of additional chemical cost.

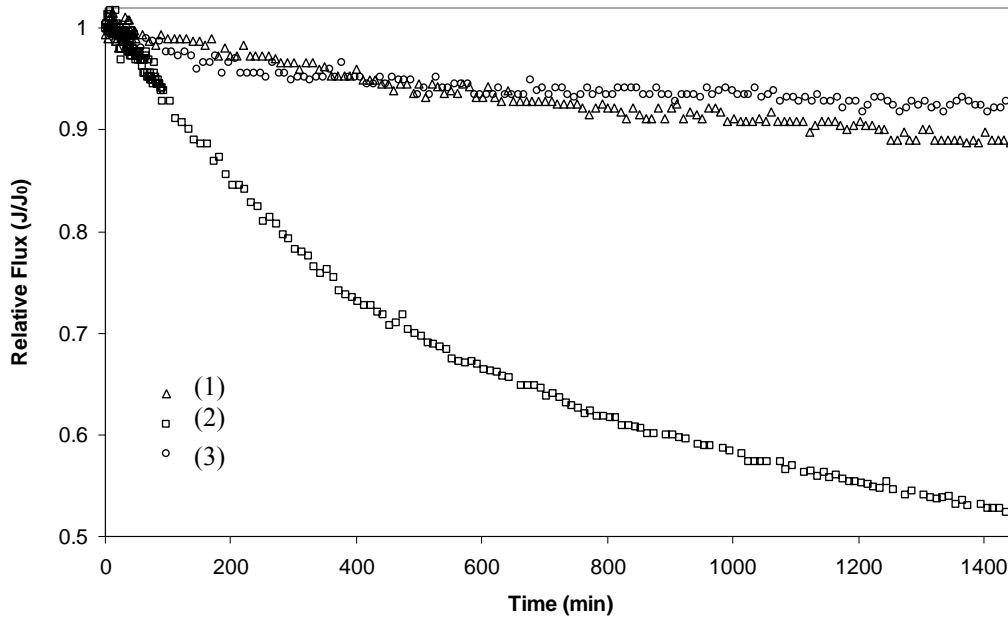


**Figure 5.5a.** Relative RO permeate flux decline tests for OAS field water sample at: (1) the native pH 7.4: 11.2% 24-hr flux decline,  $SI_{G,M0} = 2.1$ ,  $SI_{C,M0} = 5.4$ ,  $SI_{S,M0} = 0.61$ ; (2) pH 5.5: 47.4% 24-hr flux decline,  $SI_{G,M0} = 2.1$ ,  $SI_{C,M0} = 0.014$ ,  $SI_{S,M0} = 0.66$ ; and (3) pH 5.9 with 0.20 ppm antiscalant (PC-504): 7.89% 24-hr flux decline:  $SI_{G,M0} = 2.1$ ,  $SI_{C,M0} = 0.86$ ,  $SI_{S,M0} = 0.66$ .

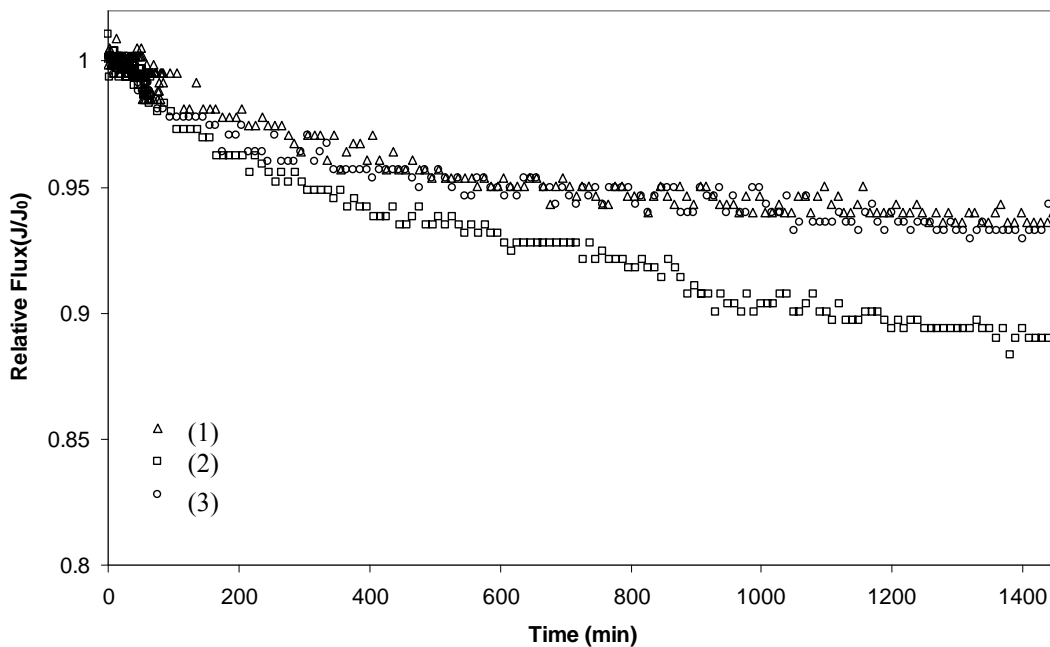


**Figure 5.5b.** Relative RO permeate flux decline tests for CNR field water sample at: (1) the native pH 7.5: 6.37% 24-hr flux decline,  $SI_{G,M0} = 1.5$ ,  $SI_{C,M0} = 7.4$ ,  $SI_{S,M0} = 0.46$ ; (2) pH 5.3: 11.0% 24-hr flux decline,  $SI_{G,M0} = 1.5$ ,  $SI_{C,M0} = 0.0061$ ,  $SI_{S,M0} = 0.49$ ; and (3) pH 6.0 with 0.20 ppm antiscalant (PC-504), 6.73% 24-hr flux decline,  $SI_{G,M0} = 1.5$ ,  $SI_{C,M0} = 0.11$ ,  $SI_{S,M0} = 0.49$ .

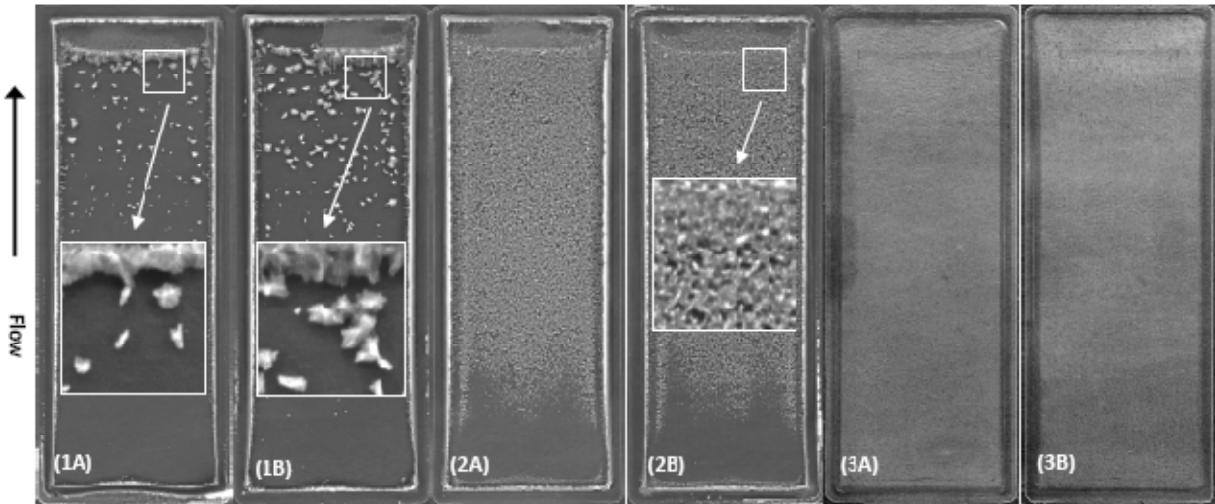


**Figure 5.6a.** Membrane coupons after 24-hour flux decline test with OAS field water at (1) the natural pH 7.42, (2) low pH 5.47, and (3) pH 5.94 with 0.20 ppm antiscalant (PC-504). Note: “A” and “B” indicate the test cell in which the coupon was placed.

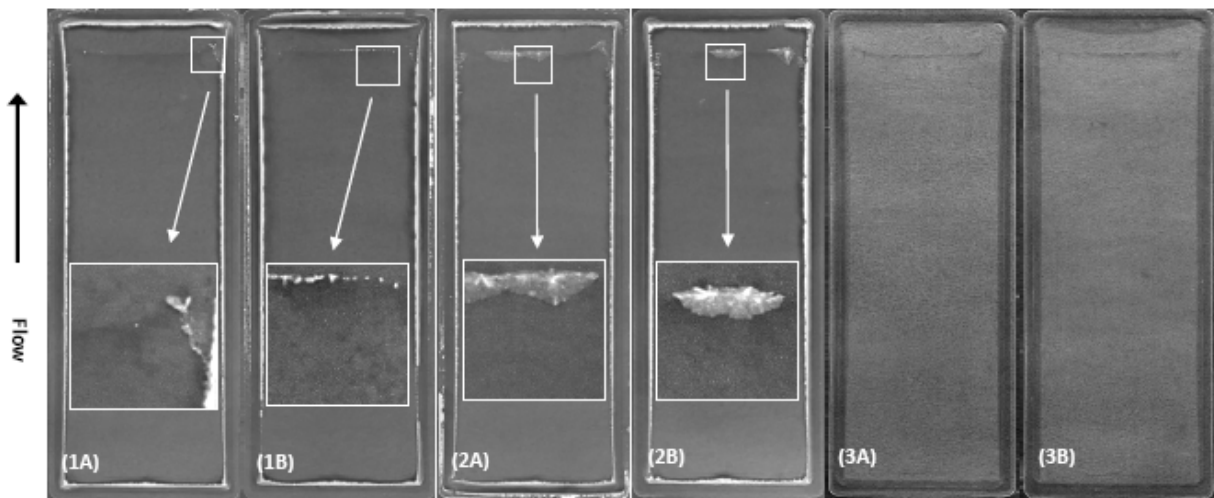


**Figure 5.6b.** Membrane coupons after 24-hour flux decline tests with CNR field water at (1), the natural pH 7.50 (2), pH 5.27, and (3) pH 6.00 with 0.20 ppm antiscalant (PC-504). Note: “A” and “B” indicate the test cell in which the coupon was placed

## 6.0. Process Analysis and Laboratory Assessment of High Water Recovery via Integration of Accelerated Precipitation Softening with RO Desalination

### 6.1 Overview

High recovery desalting of SJV AD water (at or above about 90%) would be possible through a reduction of the level of supersaturation of the mineral salt sealants of concern. Water TDS in the neighborhood of 10,000 mg/L is a common occurrence in the San Joaquin Valley (**Tables 5.1 and 5.4** and **Fig. 5.1**). The VGD site is an exception with TDS levels that are typically above 20,000 mg/L. Recent water quality analysis showed that the water at OAS and LNW are near or slightly above saturation with respect to gypsum ( $SI_g$  of 0.98 and 1.03 for OAS and LNW, respectively). Although the TDS levels for LNW (11,270 mg/L) and OAS (11,020 mg/L) are similar, supersaturation with respect to calcite at OAS ( $SI_c=3.02$ ) is higher than for the LNW site ( $SI_c=2.72$ ). Historical data revealed that at the OAS site, the highest saturation index for gypsum was encountered during 3/22/2004 sampling (**Table 5.1**). This specific water composition (hereinafter designated as OAS/E) was selected for evaluating different alternatives for enhancing RO water recovery. The technical feasibility and limitations on RO membrane desalting were investigated via process analysis/design calculations and bench-scale experiments to assess the effectiveness of accelerated precipitation softening in averting membrane scaling. The more recent water quality analysis data (**Table 5.2**) revealed that source water LNW had the highest level of gypsum saturation. Accordingly, both the above OAS and LNW water sources were considered in evaluating the technical and economic feasibility for high recovery desalting.

### 6.2 High Recovery RO of Agricultural Drainage Water from the OAS Location

#### 6.2.1 Recovery Limits

Based on the analysis method described previously (**Section 5.1.1**), the OAS/E water source can be desalinated up to a recovery level of 51% (see **Fig. 5.1**), provided that barium sulfate scaling is also mitigated by antiscalants treatment. It must be recognized, however, that osmotic pressure of the RO concentrate may also limit the achievable water recovery level. For this source water the osmotic pressure would reach about 600 psi at 90% recovery. It is noted that commercial vessels for nanofiltration (NF) and ultra-low pressure RO (ULP-RO) are typically rated for 350 psi maximum pressure limit. Low pressure RO (High rejection (HR-RO) and extra high rejection (XR-RO) modules are generally rated for a 600 psi pressure limit, while seawater desalination RO module are usually made to withstand pressure of up to about 1200 psi. Clearly, if low pressure/high rejection RO desalting is the process of choice for the OAS/E source brackish water desalination, then water recovery would be limited to about 90% (**Table 5.4**). Higher recovery (>90%) may be possible if seawater RO modules are considered.

In order to achieve product water recovery beyond that which is possible with antiscalants treatment (i.e., up to  $SI_g=2.3$  which would enable ~61% recovery), the concentration of calcium would have to be reduced to lower the saturation level with respect to gypsum. The percent calcium removal required to maintain the concentrate at just the saturation level with respect to gypsum can be determined based on multi-ion thermodynamic solubility analysis. The results of such analysis (**Fig. 6.2**) demonstrate that achieving 90% product water recovery would require about 85% calcium removal.



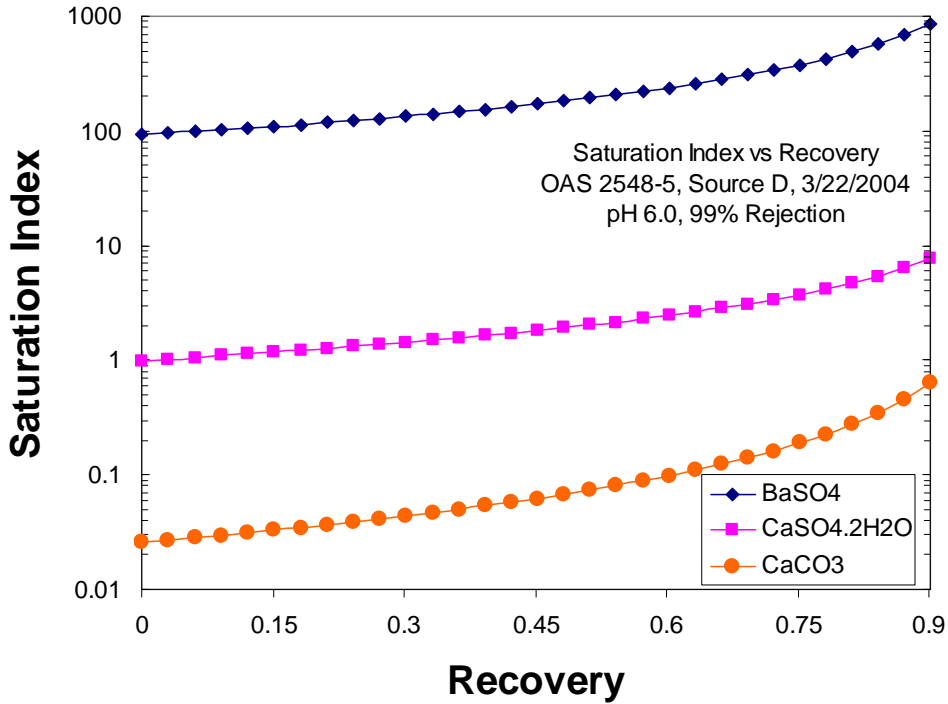


**Figure 6.1.** Dependence of mineral salt saturation indices on the level of product water recovery for membrane desalting (at 99% salt rejection) of brackish groundwater for OAS/E source water (Table 5.1).

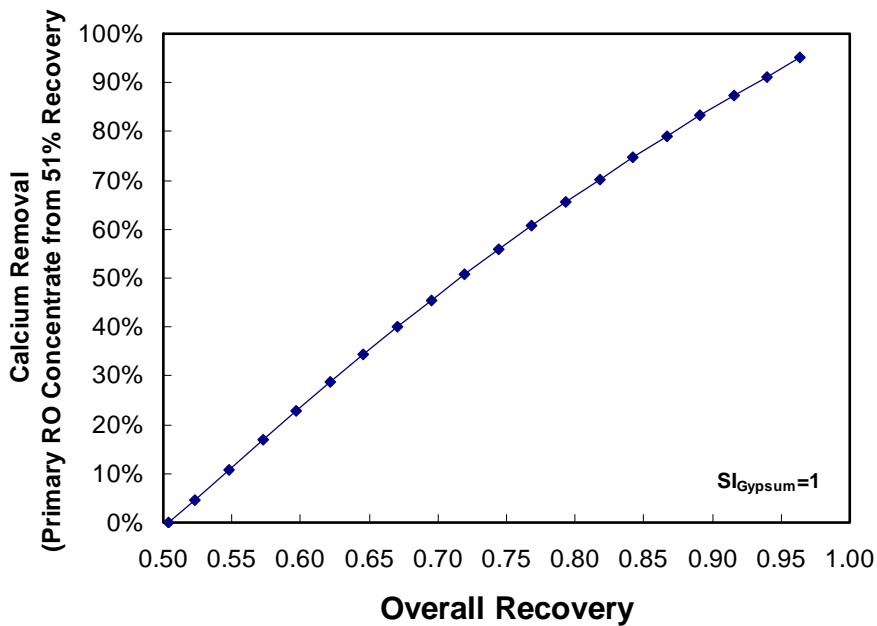


**Figure 6.2.** Process simulations of integrated RO-accelerated precipitation softening for source water OAS.

### 6.2.2 Overview of RO Process Simulations

In order to assess the technical feasibility of high recovery RO desalting two process integration alternatives that combine accelerated precipitation softening (APS) with RO membrane desalting were considered: (1) a single step RO desalination in which the feed is treated by accelerated precipitation softening (APS) followed by membrane RO desalting (**Fig. 6.3a**); and (2) a two-step membrane RO desalination in which the primary RO concentrate from a first stage RO desalination is treated by APS with a subsequent secondary RO desalting (**Fig. 6.3b**). The analysis was conducted using the ROPRO simulator (Koch Membrane Systems). For the single step APS-RO desalting process (**Fig. 6.3a**), a two stage membrane module configurations was utilized with the concentrate from the first RO stage desalted in a secondary RO stage. For the two-step APS-RO process (**Fig. 6.3b**) two different membrane stage configurations were considered: (a) a single stage RO (**Fig. 6.4a**), and (b) a two-stage RO module design (**Fig. 6.4b**). In the two stage configuration (**Fig. 6.4b**) an inter-stage pump is used to compensate for the osmotic pressure rise with increased recovery.

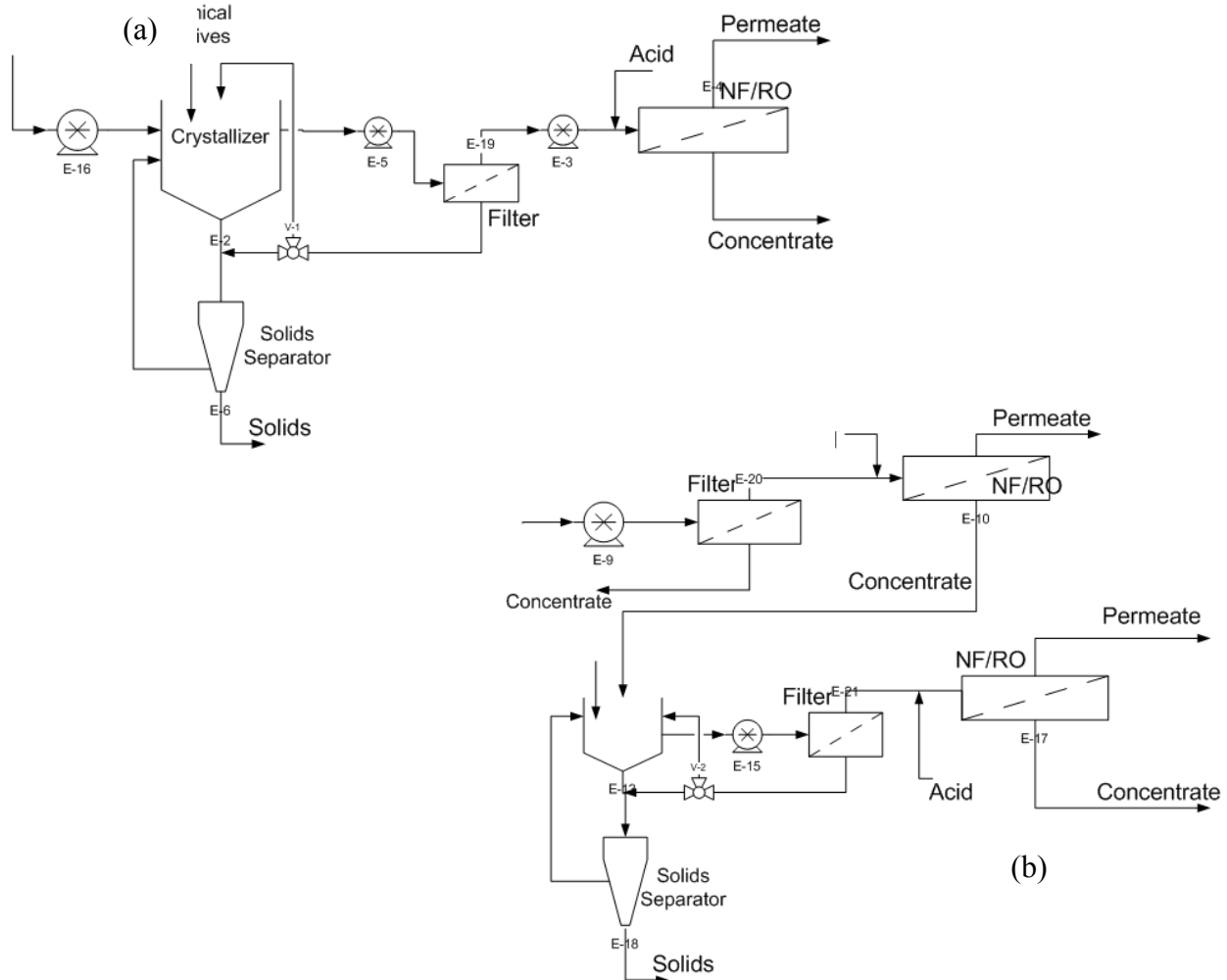


**Figure 6.3.** (a) Single step high recovery RO desalination, (b) two-step high recovery RO desalination.

RO process simulations were carried out for both the single-step and two-step strategies for a 5 MGD plant size for two overall recovery levels of 75% and 90%. The results are shown in **Tables 6.2** and **6.3**. In all cases, the final permeate quality in terms of total dissolved solids (TDS) was within the recommended limit of 750 mg/L for agricultural water utilization.

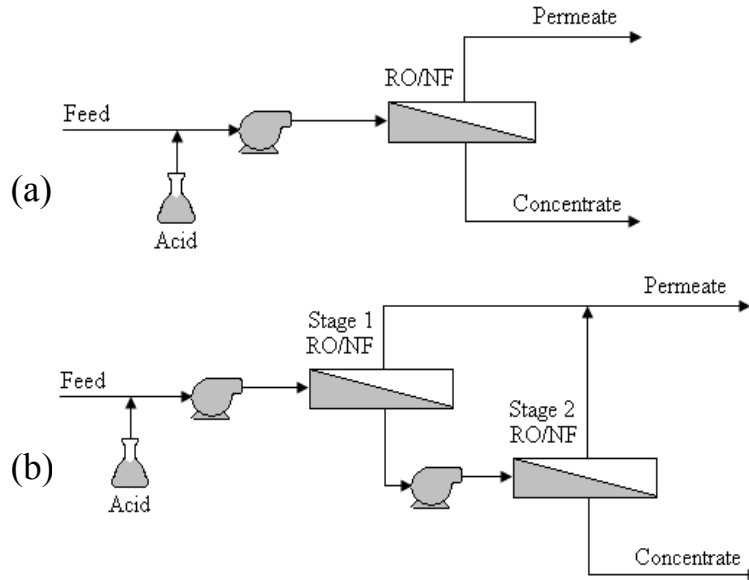


**Figure 6.4.** RO/NF stage designs: (a) Single-stage module configuration, (b) Two-stage RO module arrangement

### 6.2.3 Single Step APS-Membrane Desalting

In the single-step APS-RO desalting, accelerated precipitation softening (APS) for calcium removal was applied to the total feed volume. In the first simulation APS treatment of the feed was specified for 76% calcium removal (**Fig. 6.5a**). This level of APS treatment enabled 75% product water recovery in the membrane desalting stage while maintaining the saturation index for gypsum below unity (**Table 6.2**). Recovery of 60% was attained in the first stage with 37.6% recovery obtained in the second stage. The use of low pressure high flux RO membrane (TFC-ULP for both stages) enabled operation at pressure that did not exceed 260 psi with a concentrate of about 35 g/L TDS.

In order to increase the product water recovery level, a two-stage membrane desalting configurations was explored. Calcium removal from the feed (via APS) was specified at a level of 89% in order to meet the objective of 90% product water recovery (**Fig. 6.5b** and **Table 6.2**). The feed was first treated by APS to attain 89% calcium removal from the feed. However, in order to meet the target permeate TDS of 750 mg/L, extra high rejection RO (XR-RO) were used in both membrane stages, resulting in higher pressure requirements (430 psi for stage 1 and 560 psi for stage 2). Water recovery of 79.5% was obtained for the first stage and 51% was attained in the second stage. In the above approach the high permeate quality in the first stage compensates for the lower permeate quality in the second stage (due to the high TDS that must be handled in the second RO stage).

#### **6.2.4 Two-Step APS-Membrane Desalting**

In the two-step APS-RO process the feed was first desalted to achieve product water recovery of 54.3% (**Table 6.1**). This recovery level is possible with the application of antiscalants since the gypsum saturation index is 2.16 which is below the upper limit recommended for antiscalant application. Desalting was achieved with a single pass TFC-ULP module to achieve permeate TDS below 500 mg/L at operating pressure of 213 psi (**Table 6.1**).

In order to achieve 75% overall product water recovery the primary RO concentrate was desalted in a secondary RO treatment after first being treated by APS with specified 74% calcium removal (**Fig. 6.6a**). A single pass ULP module was also utilized operating at a pressure of 341 psi. Water recovery in this second desalting stage was at 45.3% with a concentrate TDS of about 37,000 mg/L. It is noted that operation at a lower pressure is possible by decreasing the permeate flux and increasing the number of membrane modules.

Higher product water recovery can be achieved by utilizing a two-stage module configuration for the secondary desalting step. The primary desalting step can be achieved with a TFC-ULP membrane operating at pressure of 213 psi at 54.3% product water recovery (**Fig. 6.6b** and **Table 6.2**). The primary membrane desalting concentrate (~20,500 mg/L TDS) is treated by APS to achieve a specified calcium removal of 89%. The high TDS of the primary RO concentrate requires an extra high rejection RO membrane (TFC-XR) for both stages of the secondary membrane desalting step. Product water recovery of 63% and 40.5% were attained for the first and second stages, respectively, of the secondary desalting step. This enabled 90% overall product water recovery with the first and second stage secondary RO desalting units operating at pressures of 562 psi and 638 psi, respectively (**Table 6.2**). It is noted that the operating pressure can be decreased somewhat by increasing the number of elements which would allow operating at a lower flux.

The above simulations were conducted to demonstrate the level of achievable RO recovery for a number of possible process configurations. The configurations and the operating conditions were not optimized with respect to process cost, recovery or product water quality. Notwithstanding, the analysis clearly demonstrated that even for the most difficult source water (highest saturation with respect to gypsum), high recovery is possible provided that the APS step for calcium removal is integrated with membrane desalting.

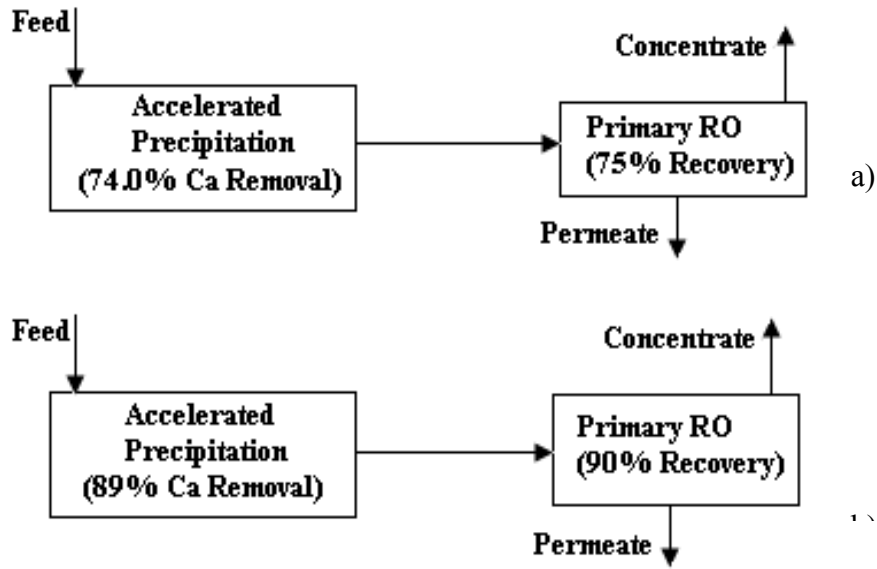


**Figure 6.5.** Single-step high recovery desalination with precipitation of the feed stream for calcium removal: (a) 75% recovery, (b) 90% recovery

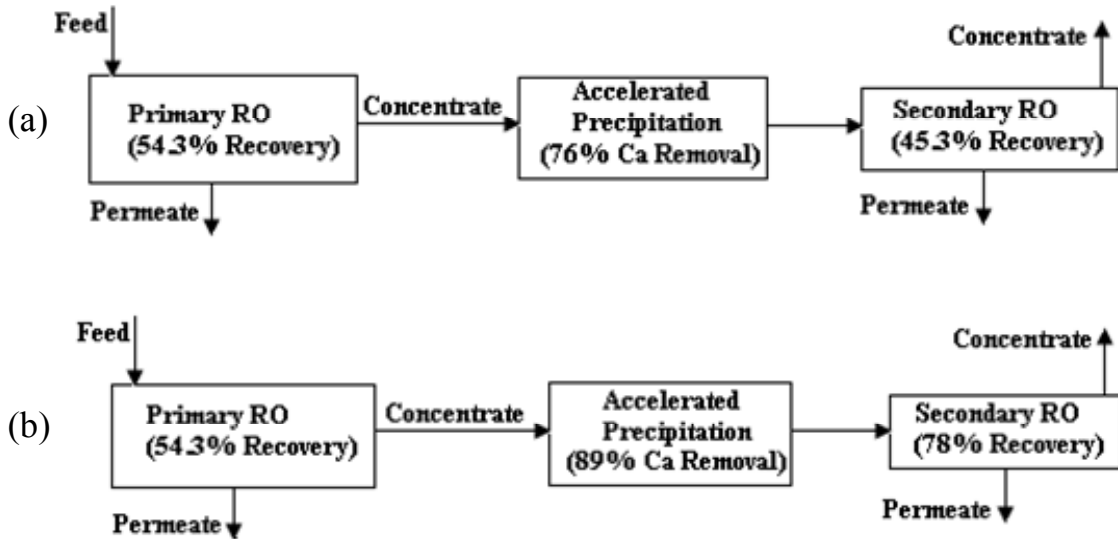


**Figure 6.6.** Two-step high recovery desalination with inter-step precipitation for calcium removal: (a) 75% recovery, (b) 90% recovery.

**Table 6.1.** Process simulation results for a single step high recovery 5 MGD desalination of agricultural drainage water (OAS site). The primary RO feed is treated by accelerated precipitation softening.

	<b>75% Recovery</b>	<b>90% Recovery</b>
<b>Membrane Stages</b>	Two Stages	Two Stages
<b>Element Type</b>	ULP-RO / NF	XR-RO / XR-RO
<b>Accelerated Precipitation</b>		
% Calcium Removal	76%	89%
<b>Feed Flow Rate (MGD)</b>	5	5
<b>Stage 1</b>		
Recovery	60%	79.5%
Pressure w/ FA (psig)	228	430
Elements per vessel	4	5
Element		
Bank 1	TFC 8823ULP-400	TFC 8822XR-400
Bank 2	TFC 8823ULP-400	TFC 8822XR-400
Number of Vessels (Permeate Flux)		
Bank 1	90 (16.9 GFD)	114 (15 GFD)
Bank 2	43 (7.8 GFD)	57 (4.9 GFD)
<b>Stage 2</b>		
Recovery	37.60%	51%
Pressure w/ FA* (psig)	254.9	563.9
Elements per vessel	5	7
Element		
Bank 1	TFC 8923S-400	TFC 8822XR-400
Bank 2	-	-
Number of Vessels (Permeate Flux)		
Bank 1	34 (11 GFD)	47 (4 GFD)
Bank 2	-	-
<b>Step TDS (mg/L)</b>		
Feed	9,764	9,765
Concentrate	36,873	9,0763
Permeate	747	721
<b>Overall Permeate TDS (mg/L)</b>	747	721
<b>Final Concentrate</b>		
Flow Rate (MGD)	1.25	0.50
$SI_{Gypsum}$	0.976752	0.95
$SI_{Calcite}$ (pH)	0.43 (pH 7.0)	0.27 (pH 6.9)
Osmotic Pressure (psi)	220	539

\* FA: Fouling Allowance = 15 % ; Feed pH was set to 6 by the addition of H<sub>2</sub>SO<sub>4</sub>

**Table 6.2.** Process simulation results for a two-step high recovery 5 MGD desalination of agricultural drainage water (OAS site). The primary RO concentrate is treated by accelerated precipitation.

	<b>Primary Step</b>	<b>Secondary Step</b> (75% Overall Recovery)	<b>Secondary Step</b> (90% Overall Recovery)
<b>Step Design</b>	Single Stage	Single Stage	Two Stages
<b>Element Types</b>	ULP-RO / NF	ULP-RO	XR-RO / HR-RO
<b>Accelerated Precipitation</b>			
% Calcium Removal	-	74%	89%
<b>Feed Flow Rate (MGD)</b>	5	2.28	2.28
<b>Water Recovery</b>			
Primary	54.3%	54.3%	54.3%
Secondary	-	45.3%	78.0%
Overall	54.3%	75%	90%
<b>Stage 1</b>			
Recovery	54.3%	45.3%	63.0%
Pressure w/ FA (psig)	213	341	562
Elements per vessel	4	6	5
Element			
Bank 1	TFC 8823ULP-400	TFC 8823ULP-400	TFC 8822XR-400
Bank 2	TFC 8923S-400	-	TFC 8822XR-400
Number of Vessels (Permeate Flux)			
Bank 1	63 (17.2 GFD)	36 (12 GFD)	40 (14.9 GFD)
Bank 2	43 (14.2 GFD)	-	20 (6.2 GFD)
<b>Stage 2</b>			
Recovery	-	-	40.50%
Pressure w/ FA* (psig)	-	-	637.9
Elements per vessel	-	-	5
Element			
Bank 1	-	-	TFC 8822HR-400
Bank 2	-	-	TFC 8822HR-400
Number of Vessels (Permeate Flux)			
Bank 1	-	-	34 (5 GFD)
Bank 2	-	-	-
<b>Step TDS (mg/L)</b>			
Feed	9651	20970	20906
Concentrate	20548	37461	91191
Permeate	481	1057	1065
<b>Overall Permeate TDS (mg/L)</b>	481	640	712
<b>Final Concentrate</b>			
Flow Rate (MGD)	2.285	1.25	0.50
$SI_{Gypsum}$	2.16	1.02	0.96
$SI_{Calcite}$ (pH)	0.62 (pH 6.8)	0.23 (pH 6.7)	0.67 (pH 7.1)
Osmotic Pressure (psi)	127	227	536

\* FA: Fouling Allowance = 15 %; Feed pH was set to 6 by H<sub>2</sub>SO<sub>4</sub> addition.

### 6.2.5. Antiscalant Effectiveness

In order to assess the effectiveness of antiscalants treatment in enabling one to reach a reasonable recovery in primary RO desalting, bulk crystallization tests were first conducted with a model OAS/E solution at 20°C (**Table 6.3**). The bulk crystallization induction time was determined following the method of Shih et al. [44]. The crystallization induction time for the feed solution (without antiscalants addition) was determined to be about 40 minutes (**Fig. 6.7a**). Upon the addition of 3 ppm of the antiscalants Flocon 100, precipitation was not observed even after a period of seven days (**Fig. 6.7b**).

**Table 6.3.** Composition of OAS Model solutions representing primary RO desalination feed and concentrate (54.3 % recovery; pH adjusted with HCl).

	Feed (mM)	Concentrate (mM)
Na <sub>2</sub> SO <sub>4</sub>	49.28	107.61
MgSO <sub>4</sub> ·7H <sub>2</sub> O	9.15	19.86
CaCl <sub>2</sub> ·2H <sub>2</sub> O	11.29	24.52
NaNO <sub>3</sub>	0.73	1.23
NaHCO <sub>3</sub>	2.91	4.39
pH	7.8	6.8*
<i>SI</i> <sub>Gypsum</sub>	0.99	2.16
<i>SI</i> <sub>Calcite</sub>	3.98	0.61

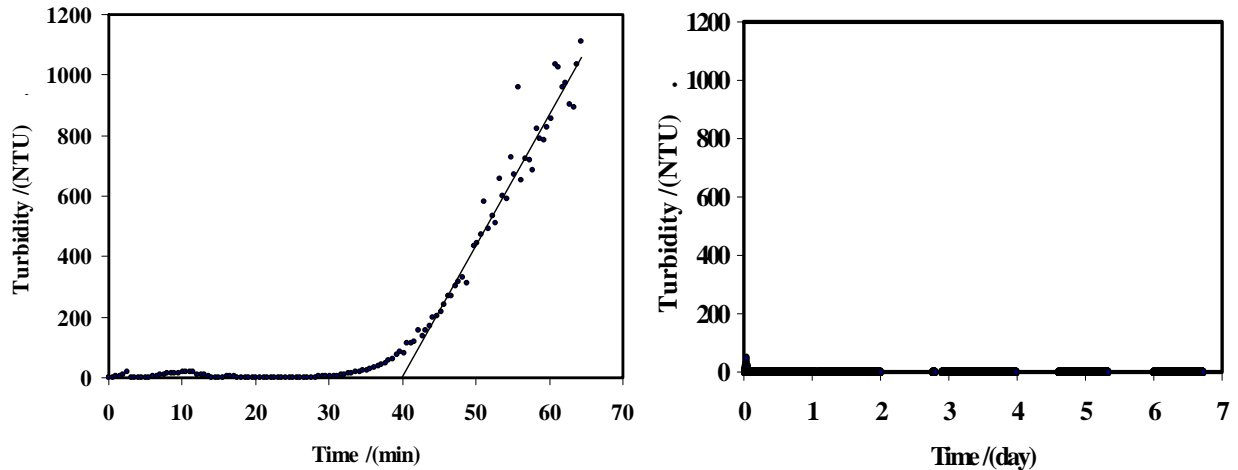


**Figure 6.7.** Bulk crystallization of OAS/E model solution at  $SI_g = 2.16$  (Brine concentrate from primary Ro at recovery of 54.3 %: a) No Antiscalant b) 3 ppm Flocon 100.



Subsequently, scaling due to surface crystallization was evaluated in a membrane scaling test with a model solution, dosed with 3 ppm antiscalants, using the dual cell plate-and-frame RO system (**Fig. 5.1**) following the method described in **Section 5.3**. The scaling test was conducted at feed cross flow velocity of 0.11 m/s and transmembrane pressure of 270 psi. At the above conditions, the average concentration polarization level (CP) was estimated to be 1.74 which resulted in an average saturation index of gypsum ( $SI_{gypsum}$ ) at the membrane surface of 1.96. The flux decline results shown in **Fig. 6.8** indicate less than 2-3% flux decline over the 24 hour test period, which is well within the experimental error of the diagnostic test. The above results demonstrated that antiscalant treatment at a dose of 3 ppm was effective in mitigating scaling. Considering that the feed convective residence time in a commercial RO system (of the order of minutes or less) is much shorter than the 24 hr test period, it is possible that a lower antiscalants dose could be applied.

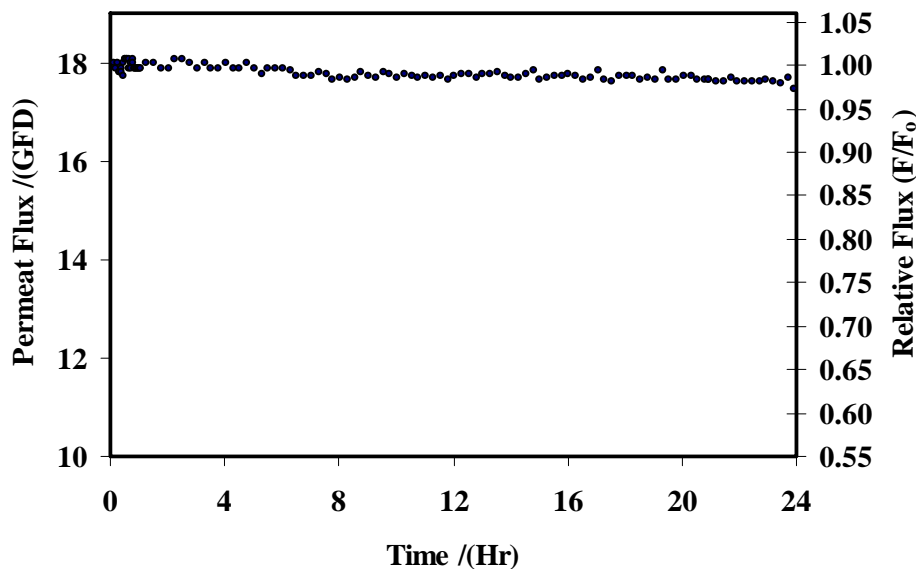


**Figure 6.8.** Membrane RO scaling test of OAS/E model solution. Initial saturation index of gypsum at the membrane surface = 1.96 (equivalent recovery of ~ 42%), 3 ppm dosage of the antiscalants Flocon 100.

### 6.2.6. Calcium Removal by Accelerated Precipitation Softening

The feasibility of calcium removal by dosing with either  $\text{Na}_2\text{CO}_3$  or  $\text{NaOH}$  was first evaluated via theoretical equilibrium calculations. The analysis was carried out for the primary RO model feed solution (**Table 6.4**) and for a primary RO concentrate obtained by RO desalting of the feed at 54.3% recovery. The theoretical results are depicted in **Fig. 6.9** in which the alkali dose refers to the addition of either  $\text{Na}_2\text{CO}_3$  or  $\text{NaOH}$ . The OAS/RO feed water is limited in terms of its carbonate concentration. Therefore, the addition of  $\text{NaOH}$  will result in calcium carbonate precipitation up to the point where the carbonate ion has been exhausted. The addition of  $\text{NaOH}$  alone is insufficient and  $\text{Na}_2\text{CO}_3$  addition is thus needed to increase the carbonate concentration. As demonstrated in **Fig. 6.9**, calcium removal can be achieved by either  $\text{Na}_2\text{CO}_3$  dosing alone or in combination with  $\text{NaOH}$ .

A series of experiments were conducted to verify the reliability of the equilibrium calculations. In the first set of studies the primary RO feed model solution (without antiscalants addition) was dosed with different amounts of  $\text{Na}_2\text{CO}_3$  along with the addition of calcite seeds at a load of 1.4 g/L. Clearly, the experimental results (**Fig. 6.10a**) are in excellent agreement with the theoretical equilibrium analysis. In a second set of experiments, the primary RO feed was dosed with 878 mg/L of  $\text{Na}_2\text{CO}_3$  so as to obtain calcium removal of about 71%, followed by the addition of sodium hydroxide. As shown in **Fig. 6.10b**, the experimental percent removal of calcium was lower (especially at higher NaOH dose) than estimated based on the equilibrium analysis. It is believed that  $\text{CO}_2$  exchange with the atmosphere in the present open precipitation system, an effect not considered in the theoretical analysis, contributed to the observed deviation.

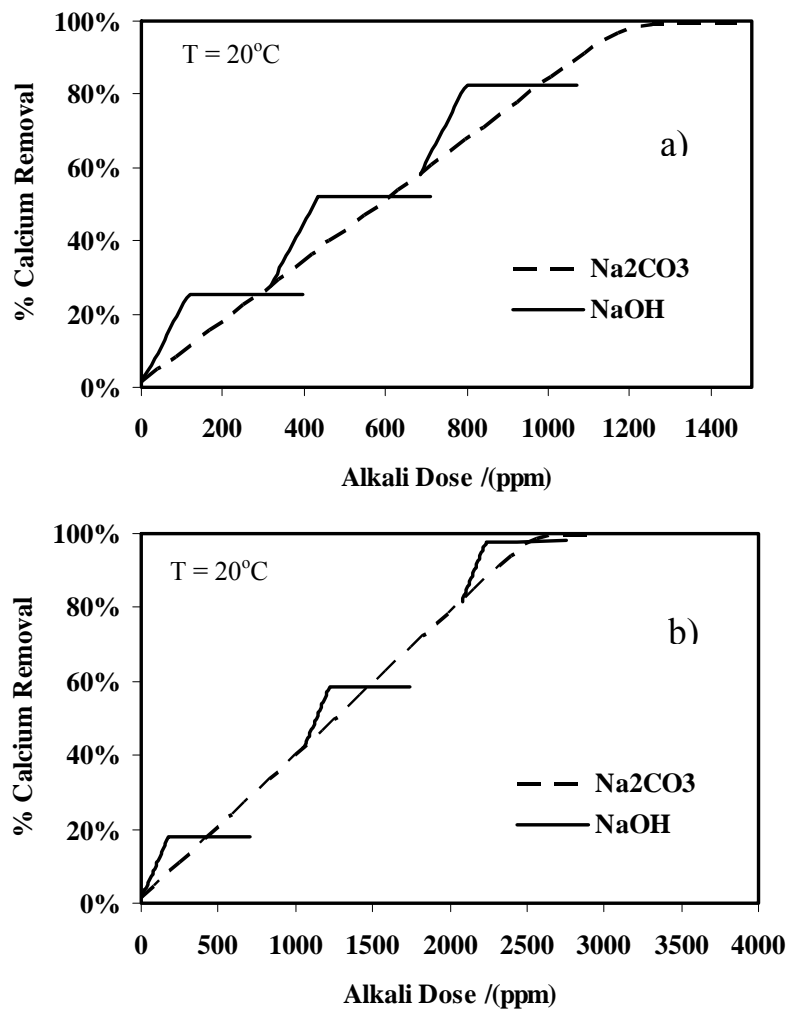


**Figure 6.9.** Theoretical equilibrium analysis of calcium removal by accelerated precipitation softening of OAS/E model solution: (a) primary RO feed, (b) primary RO concentrate from 54.3% recovery.

In order to evaluate the feasibility of calcium removal from the primary RO concentrate (produced via desalting at 54.3% water recovery), batch accelerated precipitation softening

A series of accelerated precipitation softening tests were carried out with  $\text{Na}_2\text{CO}_3$  and  $\text{NaOH}$  dosing along with calcite seeding. Antiscalant (Flocon 100) was added to the model primary RO concentrate solution (**Table 6.4**) at a dose of 6 ppm. The results of APS with  $\text{Na}_2\text{CO}_3$  dosing are in excellent agreement with the equilibrium calculations (**Fig. 6.11a**). The experimental data confirmed that antiscalants in the concentrate did not adversely affect calcium removal by APS. In a second test, the model RO concentrate was first dosed with 2,083 mg/L  $\text{Na}_2\text{CO}_3$  to achieve about 78% calcium removal, followed by  $\text{NaOH}$  dosing to calcium removal in excess of 90% (**Fig. 6.11b**). The experimental calcium removal results followed the theoretical predictions, but were consistently over predicted (1%-6%), possibly due to  $\text{CO}_2$  exchange with the atmosphere in the open experimental system.

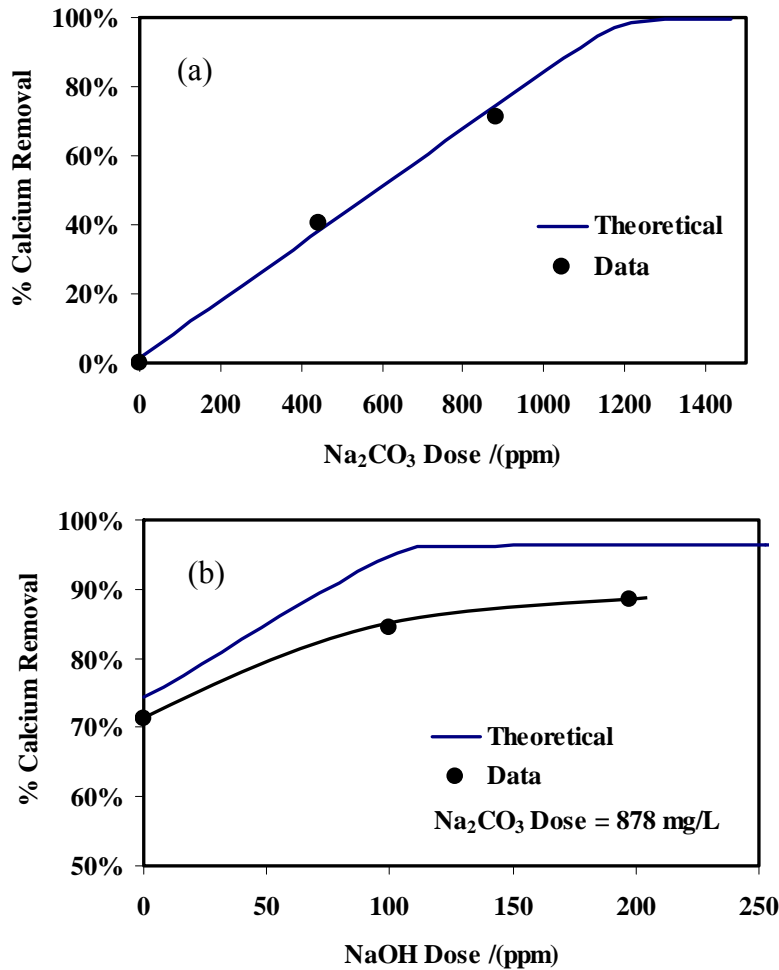


**Figure 7.10.** Calcium removal by accelerated precipitation softening of OAS/E model feed solution (**Table 6.4**). (a)  $\text{Na}_2\text{CO}_3$  dosing with calcite seed load of 1.4 g/L, (b)  $\text{NaOH}$  dosing along with the initial addition of 878 mg/L  $\text{Na}_2\text{CO}_3$  and calcite seed load of 1.4 g/L. Equilibration period= 30 hr,  $T= 20^\circ\text{C}$ .

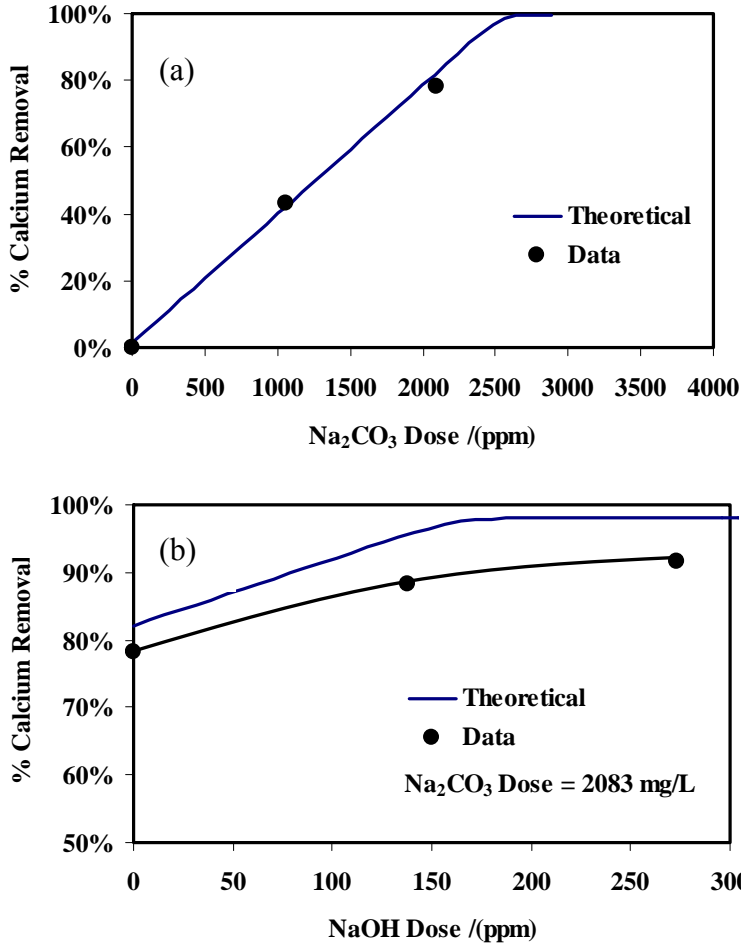


**Figure 6.11.** Calcium removal by accelerated precipitation softening (APS) of OAS/E model solution of primary RO concentrate obtained from RO desalting at recovery of 54.3%. (a)  $\text{Na}_2\text{CO}_3$  dosing with calcite seed load of 1.4 g/L, (b) NaOH dosing along with the initial addition of 2083 mg/L  $\text{Na}_2\text{CO}_3$  and calcite seed load of 1.4 g/L,  $T = 20^\circ\text{C}$ .

In order to further evaluate the feasibility of APS, the precipitation kinetics was assessed using the OAS/E model solution for the primary RO feed and the primary RO concentrate (produced at 54.4% recovery). These experiments were conducted in a 600 ml vessel in which calcium depletion was followed over the course of the precipitation process. Calcium concentrations at a given time, relative to the initial concentration, are plotted in **Figs. 6.12a** and **6.12b** for APS treatment of the primary RO and RO concentrate, respectively. Precipitation was induced by the addition of  $\text{Na}_2\text{CO}_3$  and calcite seeding of 1.4 g/L. Steady state with respect to calcium precipitation was approached within ~10-20 minutes. Steady-state calcium removal was closely predicted by the equilibrium prediction. For the primary RO concentrate, the time to reach steady state was longer than for the primary RO feed. It is noted that for the RO concentrate to which 6 ppm antiscalants was added, the experimental calcium concentration at pseudo-steady state was somewhat higher (~3%) than the equilibrium prediction. In other words, the experimental percent of calcium removal was lower than predicted. The above deviation could be due to the presence of the antiscalants which complexes with calcium nuclei and also retards crystal growth. It is possible that, over a longer period of time, the calcium concentration will decline and eventually approach the predicted equilibrium level.

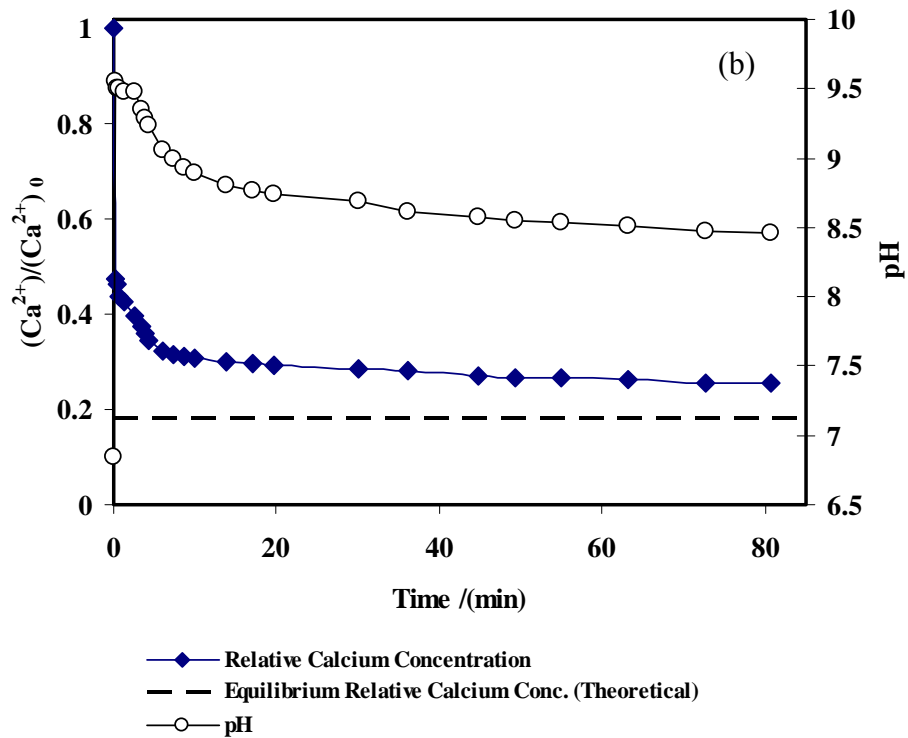
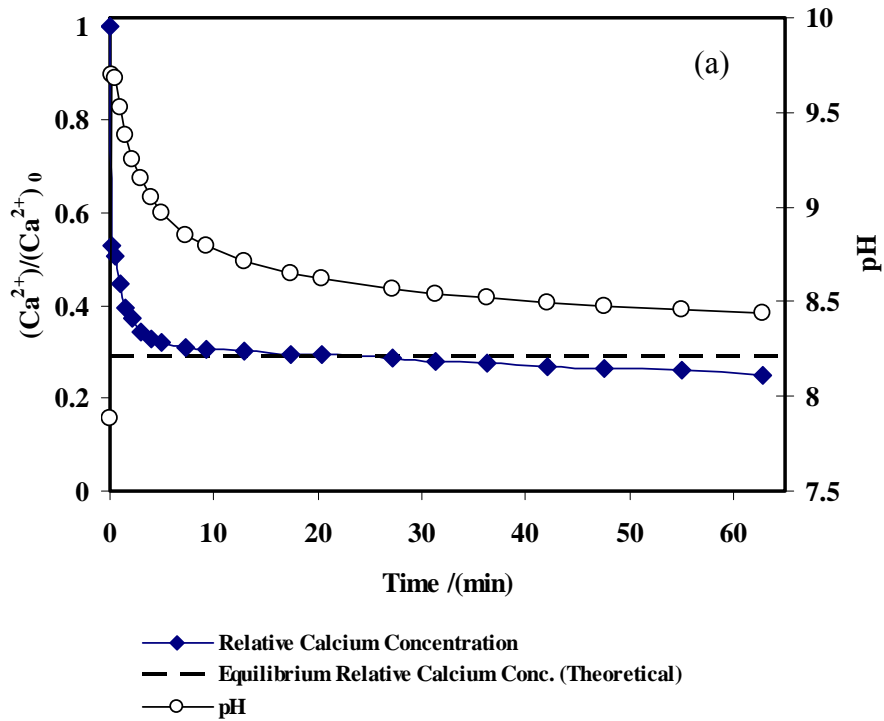


**Figure 6.12.** Kinetics of accelerated precipitation softening of OAS solutions:  
 (a) Primary RO feed (841 mg/L  $Na_2CO_3$  dosage, 1.4 g/L calcite seed load, no antiscalant),  
 (b) Primary RO concentrate (2,068 mg/L  $Na_2CO_3$  dosage, 1.4 g/L calcite seed load, 6 ppm Flocon 260 antiscalant).  $T = 24^\circ C$ .

### 6.3. Economic Feasibility of Two-Step Membrane Desalting with an Interstage Mineral Salt Precipitation

#### 6.3.1. RO Desalination with Interstage Accelerated Precipitation Softening (OAS Water Source)

A two-step RO membrane desalting process that integrates accelerated precipitation softening (APS) an interstage process (i.e., RO-APS-RO; **Fig. 6.3b**) would be more economical than a single step APS-RO (**Fig. 6.3a**) since a smaller volume would have to be treated by APS. In the RO-APS-RO the feed is pre-treated by microfiltration with pH adjustment (if needed) to suppress calcite scaling. A primary RO desalting step is then applied (with ~3 ppm antiscalants feed dosage) to achieve a recovery level of about 80%. Calcium removal is then achieved by APS in a crystallizer reactor. The treated stream is filtered to remove the mineral salt precipitate, and it is then desalted in a secondary RO (RO) to achieve the desired overall recovery.

In order to illustrate the economic merit in carrying out a two-step high recovery desalination process (**Fig. 6.3b**) a process economic analysis was first carried considering overall recovery levels ranging from 80% to 95%, for the OAS2548 source water of the composition on 9/9/2003 (**Table 5.1**). The cost analysis was based on a desalination plant that would process  $5 \times 10^6$  gallons/day feed water (5 MGD). Process simulations and costing analysis were carried out using the two interfaced membrane process simulators RO-PRO and Cost-PRO [56] with the membranes TF C-ULP, TFC-HR and TFC-XR considered in various stages of the primary and secondary RO desalting process. Equipment costs for membrane modules, pumps, piping, filters, crystallizer and control equipment were assessed based on information provided from various equipment manufacturers. Operational cost included membrane replacement based on a four year cycle, membrane cleaning, chemical additives, energy and maintenance. Energy cost was determined based on pumping costs and bulk rate cost of chemical additives (e.g., NaOH, Na<sub>2</sub>CO<sub>3</sub>, HCl, H<sub>2</sub>SO<sub>4</sub>, and antiscalants) was obtained from their respective manufacturers.

For all cases considered, the primary RO recovery was set at 80% (**Tables 6.5-6.8**). The capital cost was dominated by the primary RO step since it involved processing of 80% of the feed. The capital cost for the accelerated mineral salt precipitation step was about 30% of the total operating cost. The secondary RO step, which increased with overall product water recovery, was about 14%-23% of the total operating cost (**Table 6.5**). The capital cost associated with the AMSP was independent of the overall recovery since the volume of treated primary RO concentrate was identical for all three process configurations. The contribution of capital cost to the overall water production cost was 9%-11% (**Tables 6.4 and 6.5**). In the absence of interest charges the overall water production cost ranged from \$185/acre-ft to \$319/acre-ft with increased product water recovery from 80% to 95%, respectively (**Table 6.6**). The operating cost for AMSP increased by 12% as the overall recovery was increased from 90% to 95%, owing to the increase in chemical cost needed for greater removal of calcium from the primary RO concentrate (**Table 6.7**). The primary RO step was the dominant cost, comprising about 56%-60% of the total operating cost. Finance charges were estimated based on a 15 year amortization of the capital cost of the plant at an annual interest rate of 5.75 % (**Table 6.8**). The overall product water cost increased by about 6% when interest charges were included resulting in an overall water production cost of \$0.59-\$1.04 per 10<sup>3</sup> gal (equivalent to \$195-\$340 per acre-ft). It is interesting to note that the cost seawater (~\$2-\$3 per 10<sup>3</sup> gal) is about a factor of 2-5 higher than the estimated cost of desalination of SJ Valley brackish water.

**Table 6.5.** Capital Cost for Brackish Water Desalination by RO and RO-APS-RO<sup>(a)</sup>

Percent Product Water Recovery		Capital Cost (\$)			
Secondary RO	Percent Overall Recovery	Primary RO	APS	Secondary RO	Total Capital Cost
0%	80%	\$1,390,000	\$0	\$0	\$1,390,000
50%	90%	\$1,390,000	\$170,000	\$165,000	\$1,725,000
75%	95%	\$1,390,000	\$170,000	\$685,000	\$2,245,000

<sup>(a)</sup> Based on 5 MGD water feed. Primary RO is carried out at 80% recovery.

**Figure 6.6.** Estimated Cost of Brackish Water Desalination by integrated RO and accelerated precipitation softening (RO-APS-RO) at various levels of overall product water recovery<sup>(a)</sup>

Water Recovery			Total Capital Cost (\$)	Cost of Water Production (\$/10 <sup>3</sup> gal)			\$/ Acre-ft
Primary RO	Secondary RO	Overall Recovery		Capital Cost	Operating Cost	Total Cost	
0.8	0	80%	\$1,390,000	\$0.063	\$0.50	\$0.56	\$185
0.8	0.5	90%	\$1,725,000	\$0.070	\$0.80	\$0.87	\$284
0.8	0.75	95%	\$2,245,000	\$0.086	\$0.89	\$0.98	\$319

<sup>(a)</sup> Based on 5 MGD feed. Cost per 100 gallons or acre-ft on the basis of total permeate produced.

**Table 6.7.** Operating Cost for RO Desalting for the three RO-APS-RO process stages.

Percent Product Water Recovery		Operating Cost (\$/10 <sup>3</sup> gal)			
Secondary RO	Overall	Primary RO <sup>(a)</sup>	APS <sup>(b)</sup>	Secondary RO <sup>(c)</sup>	Total <sup>(d)</sup>
0%	80%	\$0.50	\$0	\$0	\$0.50
50%	90%	\$0.50 (\$0.45)	\$1.09 (\$0.24)	\$1.01 (\$0.11)	\$0.80
75%	95%	\$0.50 (\$0.42)	\$1.22 (\$0.26)	\$1.33 (\$0.21)	\$0.89

<sup>(a)</sup> Cost per water permeate produced in the primary RO step. <sup>(b)</sup> Cost per 10<sup>3</sup>gal of primary RO concentrate. Cost in parenthesis is per 10<sup>3</sup>gal of total product water. <sup>(c)</sup> Cost per 10<sup>3</sup>gal of secondary permeate water product. <sup>(d)</sup> Cost per total 10<sup>3</sup>gal of product water permeate produced.

**Figure 6.8.** Cost of water desalination including financial charges<sup>(a)</sup>

Water Recovery			Total Capital Cost (\$)	Cost of Water Production (\$/10 <sup>3</sup> gal)			\$/ Acre-ft
Primary RO	Secondary RO	Overall Recovery		Capital Cost	Operating Cost	Total Cost	
0.8	0	80	\$2,073,427	\$0.09	\$0.50	\$0.59	\$195
0.8	0.5	90	\$2,588,054	\$0.12	\$0.80	\$0.92	\$300
0.8	0.75	95	\$3,348,807	\$0.15	\$0.89	\$1.04	\$340

<sup>(a)</sup> Based on 5 MGD feed. Cost per 10<sup>3</sup> gallons or acre-ft of total permeate produced. Operating cost is as given in **Table 6.7**. Capital cost is amortized over 15 years at 5.75% interest rate.

An alternative to the use of accelerated chemical precipitation (ACP; also referred to as ASP), which is essentially a chemical demineralization process, is desupersaturation with respect to gypsum by employing accelerated gypsum precipitation (AGP) making use of gypsum seeding and lime (for calcium addition and pH control). The integration of AGP with a two-stage RO desalting process, with concentrate recycle from the secondary RO stage to the AGP stage, is shown in Fig. 6.13. Process analysis shows that for the OAS water source (**Table 5.2**), up to 95% recovery can be accomplished with process performance as indicated in **Fig. 6.13**. The integration of the alternative process of accelerated chemical precipitation (ACP; i.e., chemical demineralization as discussed previously) with a two-stage RO (**Fig. 6.14**) would result in lower energy consumption, but a higher cost of chemical additives (for feed treatment, alkaline adjustment in the APS and pH readjustment in the secondary RO). It is noted that the higher energy cost for the RO-AGP process is due to the pumping requirements for the recycle stream. The combined electrical energy and chemical cost for the RO-AGP process was estimated at \$0.12-0.15 per m<sup>3</sup> of permeate product water compared to about \$0.2 per m<sup>3</sup> permeate product for the RO-ACP process. It is noted that the above cost does not include capital cost and that the precise overall cost would be dependent on the range of water compositions that would be experience over the course of the desalting operation.

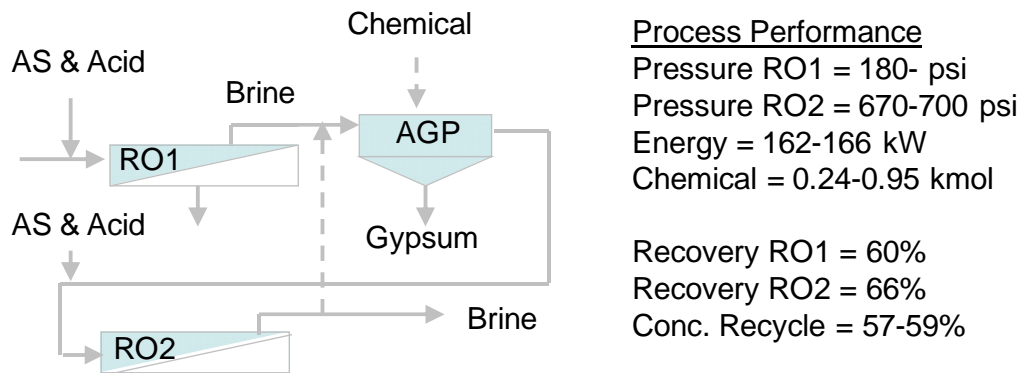


**Figure 6.13.** Implementation of high recovery desalination for feed water high in sulfate and low in silica. Feed water: OAS 2548 (9,600 mg/L, TDS), 1 MGD Feed, 9 GFD permeate flux. Target: 95% overall recovery with permeate quality of <500 mg/L.

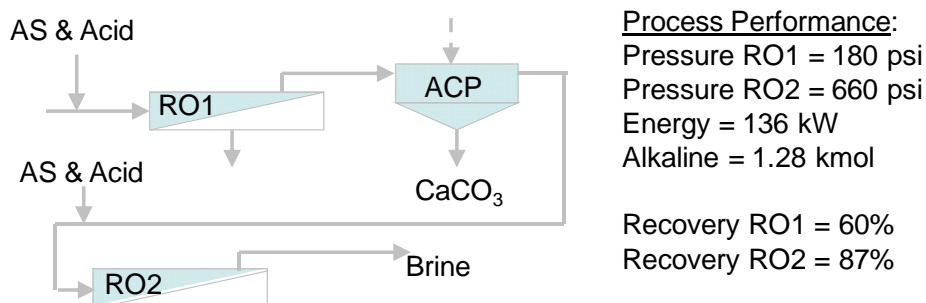


**Figure 6.14.** Process simulation for high recovery desalting with ACP integration. Feed water: OAS 2548 (9,600 mg/L, TDS), 1 MGD Feed, 9 GFD permeate flux. Target: 95% overall recovery with permeate quality of <500 mg/L.



### 6.3.2. High Recovery Desalting Analysis for the LNW Source Water

Water quality analysis for five sites in the San Joaquin Valley for the 2006-2007 season revealed that the LNW site had the highest level of gypsum supersaturation (**Table 5.3**). Therefore, this source water was the basis for further analysis of desalting potential for this high scaling propensity SJV drainage water. RO desalting with the use of antiscalants would at best enable recovery of up to 54% (**Table 6.4**). In order to achieve higher recovery, the scaling propensity of this water must be reduced by removing scale precursor ions such as calcium. The required level of calcium removal and pH adjustment to keep the calcite saturation index at 3 (with antiscalant control) necessary to attain the desired overall recovery is shown in **Fig. 6.15**. For example, to attain 90% product water recovery would require ~90% removal of calcium along with the use of antiscalants to suppress scaling of both gypsum (up to  $SI_g=2.3$ ) and calcite (up to  $SI_c \approx 3$ ).

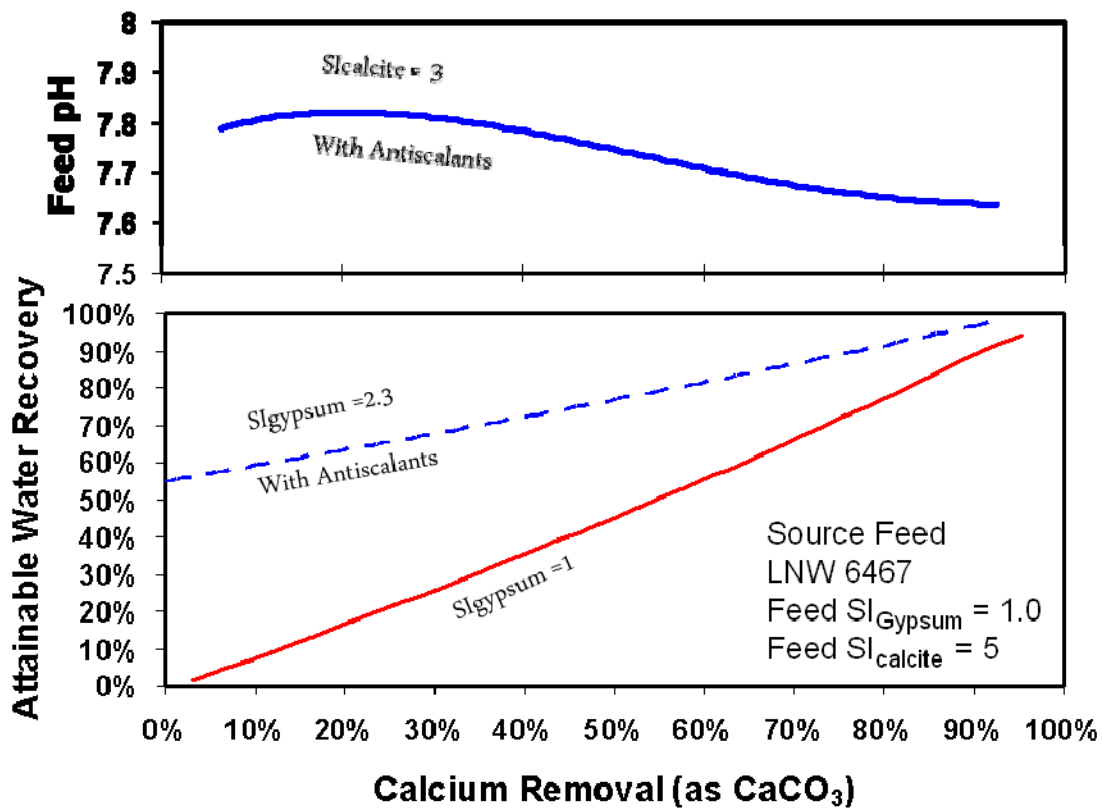


**Figure 6.15.** Calcium removal requirement and pH adjustment for high recovery desalting of LNW water (**Tables 5.2**).

In order to evaluate the potential for calcium removal by chemical demineralization (i.e., precipitation softening), the LNW field water was demineralized by the addition of  $\text{Na}_2\text{CO}_3$ . Excellent agreement was obtained between the experimentally determined calcium removal and that which was estimated based on theoretical thermodynamic solubility analysis (**Fig. 6.16a**). In this example, 91% calcium removal would be needed to achieve scale-free 90% overall RO recovery. Although this specific approach is not optimal for SJV drainage water (given the cost of sodium bicarbonate), this example does show that there was no interference from other ions or natural organic carbon. The kinetics of calcium removal for the same example is shown in **Fig. 6.16b** with and without seeding with calcium carbonate crystals. In the absence of seeding two regimes are observed – a homogenous crystallization region followed by rapid heterogeneous crystallization. The kinetics of crystallization with seeding is more rapid, but in all cases the essentially the same final equilibrium state is reached.

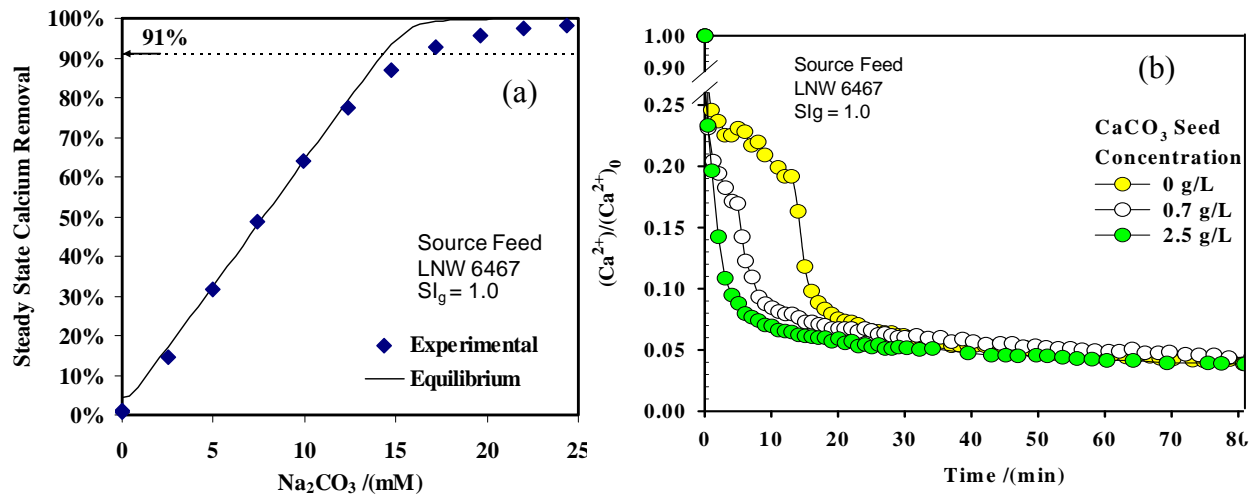


**Figure 6.16.** (a) Predicted calcium removal with the addition of sodium bicarbonate for LNW 6467 Water. (b) Calcium removal kinetics by accelerated chemical precipitation.

## 6. CONCLUSIONS

The technical and economic feasibility of RO desalting of San Joaquin Valley drainage water was evaluated in a systematic study. Analysis of historical water quality data and of recently obtained water field samples, from various locations in the San Joaquin Valley, demonstrated a significant variability of water salinity and scaling propensity with respect to calcite, gypsum, barite and silica. The above analysis and experimental RO scaling tests suggested that the expected range of product water recovery by RO desalting across the SJV can be in the range of 50%-70% for most of the sites, with the exception of the ERR site for which a much higher recovery was estimated (in excess of 90%). The integration of accelerated precipitation with RO desalting was shown to be technically feasible for the range of brackish water quality in the San Joaquin Valley. In this process the concentrate from primary RO (PRO) desalting would be treated by accelerated precipitation softening (i.e., chemical demineralization) or desupersaturated to lower the scaling propensity of this stream, followed by secondary RO (SRO) desalting. Overall recovery of up to ~90%-95% could be achieved at an estimated cost of \$0.56 -\$0.98 per m<sup>3</sup> product water, with the ACP process accounting for about 15%-25% of the overall water production cost.

It is expected that, the methods developed in the present study for scale characterization, evaluation of accelerated precipitation effectiveness and RO process performance analysis will significantly advance the knowledge base needed to arrive at optimal design and deployment of future RO desalination for the range of challenging agricultural drainage water in the San Joaquin Valley drainage.

## 7. REFERENCES

- [1] DWR, San Joaquin Valley, Drainage Monitoring Program Database, State of California, The Resources Agency, Department of Water Resources, San Joaquin District, 2003.
- [2] Evaluation of the 1990 Drainage Management Plan for the Westside San Joaquin Valley, California, San Joaquin Valley Drainage Implementation Program and University of California Ad Hoc Coordination Committee, 2000.
- [3] C. Gabelich, T. Yun, B. Coffey, and I.H. Suffet, Pilot-scale testing of reverse osmosis using conventional treatment and microfiltration, *Desalination*, 154 (2003) 207.
- [4] M.A. Clinton Williams, Agricultural Drainage in the San Joaquin Valley: A Gap Analysis, San Joaquin Valley Drainage Implementation Program, 2002.
- [5] Desalination Demonstration Report for Buena Vista Water Storage District, (2003).
- [6] S. Gao, K.K. Tanji, R.A. Dahlgren, J. Ryu, M.J. Herbel, and R.M. Higashi, Chemical status of selenium in evaporation basins for disposal of agricultural drainage, *Chemosphere*, 69 (2007) 585.
- [7] R.J. Petersen, Composite Reverse-Osmosis and Nanofiltration Membranes, *J. Membr. Sci.*, 83 (1993) 81.
- [8] A. Brehant, V. Bonnelye, and M. Perez, Comparison of MF/UF pretreatment with conventional filtration prior to RO membranes for surface seawater desalination, *Desalination*, 144 (2002) 353.
- [9] P. Cote, J. Cadera, J. Coburn, and A. Munro, A new immersed membrane for pretreatment to reverse osmosis, *Desalination*, 139 (2001) 229.

- [10] S. Ebrahim, M. Abdel-Jawad, S. Bou-Hamad, and M. Safar, Fifteen years of R&D program in seawater desalination at KISR part I. Pretreatment technologies for RO systems, *Desalination*, 135 (2001) 141.
- [11] J.C. Kruithof, J.C. Schippers, P.C. Kamp, H.C. Folmer, and J.A.M.H. Hofman, Integrated multi-objective membrane systems for surface water treatment: pretreatment of reverse osmosis by conventional treatment and ultrafiltration, *Desalination*, 117 (1998) 37.
- [12] R.Y. Ning, T.L. Troyer, and R.S. Tominello, Chemical control of colloidal fouling of reverse osmosis systems, *Desalination*, 172 (2005) 1.
- [13] T.F. Speth, A.M. Gusses, and R. Scott Summers, Evaluation of nanofiltration pretreatments for flux loss control, *Desalination*, 130 (2000) 31.
- [14] Y. Taniguchi, An overview of pretreatment technology for reverse osmosis desalination plants in Japan, *Desalination*, 110 (1997) 21.
- [15] M. Wilf and K. Klinko, Improved performance and cost reduction of RO seawater systems using pretreatment, *Membrane Tech.*, 113, 1999 (1999).
- [16] C. Gabelich, T.I. Yun, J.F. Green, I.H. Suffet, and W.R. Chen, Evaluation of precipitative fouling for Colorado River Water desalination using reverse osmosis, U.S. Department of the Interior, Bureau of Reclamation Denver, CO 80225, DWPR No. 85, December 2002.
- [17] A. Rahardianto, J. Gao, C.J. Gabelich, M.D. Williams, and Y. Cohen, High recovery membrane desalting of low-salinity brackish water: Integration of accelerated precipitation softening with membrane RO, *Journal of Membrane Science*, 289 (2007) 123.
- [18] C.J. Gabelich, T. Yun, B. Coffey, and I.H. Suffet, Pilot-scale testing of reverse osmosis using conventional treatment and microfiltration, *Desalination*, 154 (2003) 207.
- [19] R.-W. Lee, J. Glater, Y. Cohen, C. Martin, K. Kovac, M.N. Milobar, and D.W. Bartel, Low-pressure RO membrane desalination of agricultural drainage water, *Desalination*, 155 (2003) 109.
- [20] A. Rahardianto, C.J. Gabelich, M.D. Williams, J.C. Franklin, and Y. Cohen, High-Recovery Reverse Osmosis Using Intermediate Chemical Demineralization, *Journal of Membrane Science*, 301 (2007) 131.
- [21] C.J. Gabelich, T.I. Yun, M.R. Cox, C.R. Bartels, J.F. Green, and I.H. Suffet. *Evaluating Ultra-Low Pressure Reverse Osmosis for Surface Water Desalination*. in *AWWA Technology Conference*. 1999. Long Beach, CA.
- [22] E. Lyster and Y. Cohen, Numerical study of concentration polarization in a rectangular reverse osmosis membrane channel: Permeate flux variation and hydrodynamic end effects, *Journal of Membrane Science*, 303 (2007) 140.
- [23] A.L. Zydney, Stagnant film model for concentration polarization in membrane systems, *Journal of Membrane Science*, 130 (1997) 275.
- [24] OLI, *OLI Analyzer 2.0*. 2005, OLI Systems, Morris Plains, NJ.
- [25] I. Bremere, M. Kennedy, P. Michel, R. van Emmerik, G.J. Witkamp, and J. Schippers, Controlling scaling in membrane filtration systems using a desupersaturation unit, *Desalination*, 124 (1999) 51.
- [26] I. Bremere, M.D. Kennedy, A. Johnson, R. van Emmerik, G.J. Witkamp, and J.C. Schippers, Increasing conversion in membrane filtration systems using a desupersaturation unit to prevent scaling, *Desalination*, 119 (1998) 199.
- [27] J. Gilron, D. Chaikin, and N. Daltrophe, Demonstration of CAPS pretreatment of surface water for RO, *Desalination*, 127 (2000) 271.

- [28] A. Graveland, J.C. Vandijk, P.J. Demoel, and J. Oomen, Developments in Water Softening by Means of Pellet Reactors, *Journal American Water Works Association*, 75 (1983) 619.
- [29] R.C. Harries, A Field Trial of Seeded Reverse-Osmosis for the Desalination of a Scaling-Type Mine Water, *Desalination*, 56 (1985) 227.
- [30] G.J.G. Juby and C.F. Schutte, Membrane life in a seeded-slurry reverse osmosis system, *Water SA*, 26 (2000) 239.
- [31] O. Kedem and J. Ben-Dror, *Water softening process. US Patent No. 5,152,904*. 1992.
- [32] O. Kedem and G. Zalmon, Compact accelerated precipitation softening (CAPS) as a pretreatment for membrane desalination .1. Softening by NaOH, *Desalination*, 113 (1997) 65.
- [33] Y. Oren, V. Katz, and N.C. Daltrophe, Improved compact accelerated precipitation softening (CAPS), *Desalination*, 139 (2001) 155.
- [34] R. Rautenbach and T. Linn, High-pressure reverse osmosis and nanofiltration, a "zero discharge" process combination for the treatment of waste water with severe fouling/scaling potential, *Desalination*, 105 (1996) 63.
- [35] R. Rautenbach and K. Voenkaul, Pressure driven membrane processes -- the answer to the need of a growing world population for quality water supply and waste water disposal, *Separation and Purification Technology*, 22-23 (2001) 193.
- [36] S. Seewoo, R. Van Hille, and A. Lewis, Aspects of gypsum precipitation in scaling waters, *Hydrometallurgy*, 75 (2004) 135.
- [37] J.T.M. Sluys, D. Verdoes, and J.H. Hanemaaijer, Water treatment in a membrane-assisted crystallizer (MAC), *Desalination*, 104 (1996) 135.
- [38] C. Vanderveen and A. Graveland, Central Softening by Crystallization in a Fluidized-Bed Process, *Journal American Water Works Association*, 80 (1988) 51.
- [39] M. Williams, R. Evangelista, and Y. Cohen. *Non-thermal process for recovering reverse osmosis concentrate: process chemistry and kinetics*. in *Proceedings of the 2002 AWWA Water Quality Technology Conference*. 2002. Seattle, WA.
- [40] AWWA, *Water Quality and Treatment : a Handbook of Community Water Supplies*, 5th ed, ed. R.D. Letterman. McGraw-Hill, New York, 1999
- [41] R.E. Loewenthal, H.N.S. Wiechers, and G.V.R. Marais, *Softening and Stabilization of Municipal Waters*. Water Research Commission of South Africa, Pretoria, 1986
- [42] C.Y. Tai, W.C. Chien, and C.Y. Chen, Crystal growth kinetics of calcite in a dense fluidized-bed crystallizer, *Aiche Journal*, 45 (1999) 1605.
- [43] A. Almulla, M. Eid, P. Cote, and J. Coburn, Developments in high recovery brackish water desalination plants as part of the solution to water quantity problems, *Desalination*, 153 (2003) 237.
- [44] W.-Y. Shih, K. Albrecht, J. Glater, and Y. Cohen, A dual-probe approach for evaluation of gypsum crystallization in response to antiscalant treatment, *Desalination*, 169 (2004) 213.
- [45] OLI, *OLI Analyzer 2.0*. 2006, OLI Systems, Morris Plains, NJ.
- [46] Hydranautics, *Chemical Pretreatment of RO/NF*, Technical Application Bulletin No. 111 Rev. B, 2003.
- [47] R.Y. Ning, Discussion of silica speciation, fouling, control and maximum reduction, *Desalination*, 151 (2002) 67.
- [48] Kurt Kovac, Jose Faria, Tony Lam, and D. Lara, *Drainage water samples and laboratory reports*, Brian C McCool and Y. Cohen, Editors. 2006-2007: Los Angeles, CA.

- [49] AWWA, Standard Methods for the Examination of Water and Wastewater, 20th ed., American Public Health Association, Washington, DC, 1998
- [50] A. Rahardianto, W.-Y. Shih, R.-W. Lee, and Y. Cohen, Diagnostic characterization of gypsum scale formation and control in RO membrane desalination of brackish water, *Journal of Membrane Science*, 279 (2006) 655.
- [51] DWR, San Joaquin Valley, Drainage Monitoring Program 2000, State of California, The Resources Agency, Department of Water Resources, San Joaquin District, 2003.
- [52] S.F.E. Boerlage, M.D. Kennedy, I. Bremere, G.J. Witkamp, J.P. van der Hoek, and J.C. Schippers, Stable barium sulphate supersaturation in reverse osmosis, *Journal of Membrane Science*, 179 (2000) 53.
- [53] S.F.E. Boerlage, M.D. Kennedy, I. Bremere, G.J. Witkamp, J.P. Van der Hoek, and J.C. Schippers, The scaling potential of barium sulphate in reverse osmosis systems, *Journal of Membrane Science*, 197 (2002) 251.
- [54] S. He, J.E. Oddo, and M.B. Tomson, The Nucleation Kinetics of Barium Sulfate in NaCl Solutions up to 6 m and 90°C, *Journal of Colloid and Interface Science*, 174 (1995) 319.
- [55] A. Rahardianto and Y. Cohen, Kinetics and Control of Membrane Mineral Scaling in RO Desalting of Agricultural Drainage Water of High Gypsum Precipitation Potential, *Environmental Science and Technology*, in press, (2007).
- [56] *Koch Membrane Systems, ROPRO Reverse Osmosis System Design Software.*

### **Project Publications**

1. A. Rahardianto and Y. Cohen, Kinetics and Control of Membrane Mineral Scaling in RO Desalting of Agricultural Drainage Water of High Gypsum Precipitation Potential, *Environmental Science and Technology*, in press, (2007).
2. Rahardianto, A., J. Gao, C. J. Gabelich, M. D. Williams and Y. Cohen, "High recovery membrane desalting of low-salinity brackish water: Integration of accelerated precipitation softening with membrane RO," *J. Membrane Science*, 289, 123–137 (2007).
3. Lyster, E and Y. Cohen, "Numerical study of concentration polarization in a rectangular reverse osmosis membrane channel: Permeate flux variation and hydrodynamic end effects," *J. Membrane Science*, 303, 140-153 (2007).
4. Anditya Rahardianto, Wen-Yi Shih, Ron-Wai Lee and Y. Cohen, "Diagnostic characterization of gypsum scale formation and control in RO membrane desalination of brackish water," *J. Membrane Science*, 279, 655-668 (2006).
5. Shih, W-Y, J. Gao, A. Rahardianto, J. Glater, Y. Cohen and C. J. Gabelich, "Ranking of antiscalant performance for gypsum scale suppression in the presence of residual aluminum," *Desalination*, 196, 280–292 (2006).